NASA TECHNICAL NOTE

NASA TN D-3844

NASA TN D-3844

MATRIX ANALYSIS OF LONGITUDINAL AND TORSIONAL VIBRATIONS IN NONUNIFORM MULTIBRANCH BEAMS

by Robert T. Wingate

Langley Research Center

Langley Station, Hampton, Va.

NATIONAL AERONAUTICS AND SPACE ADMINISTRATION • WASHINGTON, D. C. • FEBRUARY 1967

NASA TN D-3844

MATRIX ANALYSIS OF LONGITUDINAL AND TORSIONAL VIBRATIONS IN NONUNIFORM MULTIBRANCH BEAMS

By Robert T. Wingate

Langley Research Center
Langley Station, Hampton, Va.

NATIONAL AERONAUTICS AND SPACE ADMINISTRATION

For sale by the Clearinghouse for Federal Scientific and Technical Information
Springfield, Virginia 22151 – Price $2.00

MATRIX ANALYSIS OF LONGITUDINAL AND TORSIONAL VIBRATIONS IN NONUNIFORM MULTIBRANCH BEAMS

By Robert T. Wingate
Langley Research Center

SUMMARY

Since longitudinal modes and frequencies provide basic data for dynamic analyses of arbitrary beam-like structures and since closed-form solutions for the modes are generally not feasible to obtain, an approximate method is developed for computing the natural frequencies and the corresponding mode shapes for a variable-section, unconstrained multibranch beam.

A lumped mass analogy employing influence coefficients is used to represent the beam. The simultaneous equations of motion for the lumped mass system are derived in matrix form and algebraically manipulated to yield a classical eigenvalue equation solvable by standard procedures. The orthogonality relationship of the natural modes is derived and used to form the basis of an orthogonal sweeping process for determination of modes above the fundamental.

Numerical examples including an application to a solid-fuel launch system are presented. Also, a detailed discussion is devoted to the theoretical verifications of the approximate modes and frequencies.

INTRODUCTION

The capability to calculate the longitudinal natural frequencies and associated mode shapes of beam-like structures, such as solid-fuel launch-vehicle systems, railroad trains, machine shafts, and piles, is of basic importance. The natural frequencies provide necessary design information and the modal functions, because of their special orthogonal properties, are ideal for use in "series" solutions to the differential equations of motion. Such "series" or "normal mode" solutions provide a powerful mathematical tool for the analysis of transient or steady-state response of a structure to disturbing forces.

For purposes of calculating the frequencies and mode shapes, slender structures of the type mentioned are usually represented as a simple beam which may have a varying, even discontinuous, cross section. However, for structures carrying elastic appendages

(e.g., a launch vehicle with a flexible payload within a flexible heat shield) it is sometimes necessary to represent the structure as a branched beam – that is, a main beam with subsidiary beams attached at points along its axis.

Exact solutions for the longitudinal frequencies of even a simple beam are not feasible except for very special cases of the cross-sectional variation (the solution for a constant cross section is, of course, well known). In reference 1 Bessel function solutions were obtained for a limited number of variable-cross-section beams with free-free ends and fixed-free ends. Also, in reference 2 Bessel function solutions were obtained for a fixed-free beam with a linearly varying cross section. In practical work, however, recourse is generally to approximate solutions.

The purpose of this paper is to present an approximate method for computing the longitudinal natural frequencies and mode shapes for a general variable-cross-section, multibranch beam. The method is derived for free or unconstrained beams; however, the extension of this procedure to other boundary conditions is straightforward. Through a change of variables the derived equations are also applicable to torsional problems in which the branch beams are everywhere concentric with the main beam.

Available approximate methods for the calculation of frequencies and modes of structures are voluminous, but literature on their application to longitudinal vibrations of multibranch structures is scant. The longitudinal vibrations of beams have been treated in several papers (e.g., ref. 3) by the so-called "stiffness" matrix approach in which the beam is idealized as a number of point masses connected by springs. The simultaneous equations of motion for the point masses, when written in matrix form, yield a classical eigenvalue problem which is solvable by standard methods. This approach is efficient when it works but suffers from the disadvantage that the lower frequencies, which are generally of prime interest, are associated with the subdominant eigenvalues. The author's experience, as well as that of others (ref. 4), has shown that matrix eigenvalue problems break down in the computation of the subdominant eigenvalues whenever they become small in comparison with the dominant eigenvalue.

The spring-mass idealization of a structure has also been utilized (e.g., ref. 5) to analyze longitudinal vibrations by a method associated with Holzer (ref. 6). This approach has an advantage for structures with many discontinuities in the stiffness and mass in that, through a recurrence equation, a very large number of mass points may be used without storing a large matrix in the computer. A fine definition of the mode shape can thus be obtained. It has the disadvantage that it is prone to roundoff error and other loss of numerical significance especially in the higher modes. Also, close attention is required to avoid missing modes in the trial and error search for frequencies, and a large number of iterations are required to cover the frequency spectrum of all the modes.

The method presented in this paper is a "flexibility" or influence coefficient matrix approach for the analysis of natural longitudinal or torsional vibrations of a multibranch beam. This method, which was originally developed in reference 7, is an adaptation of a procedure described in reference 8 for computing the lateral bending modes and frequencies of a single beam. It is attractive because of simplicity in derivation and its adaptability to digital programing. The major advantage, however, is that the lower frequencies are associated with the dominant eigenvalues and potential problems of accuracy loss in the lower modes and other losses in numerical significance are virtually eliminated. The development is completely general and requires only basic parameter changes from one application to another.

By proceeding from basic physical assumptions, simple matrix algebra is used to obtain the characteristic equation in matrix form. Iterative procedures for obtaining the frequencies and modes are then discussed. Numerical examples are given for an idealized beam and a typical solid-fuel launch vehicle to illustrate the formulation and solution of the derived matrix equations. Also, a detailed discussion is devoted to the accuracy of the method in comparison with exact solutions and solutions by the "stiffness" matrix approach.

SYMBOLS

A	stressed cross-sectional area, inches^2 (meters^2)
$A(j)$	stressed cross-sectional area of jth branch, a function of x, inches^2 (meters^2)
E	Young's modulus, pounds force/inch^2 (newtons/meters^2)
$E(j)$	Young's modulus of jth branch, a function of x, pounds force/inch^2 (newtons/meter^2)
$F_{r(j)}, F_{s(k)}$	axial force at $x_{r(j)}$, $x_{s(k)}$, pounds force (newtons)
$G_{r(j),s(k)}$	influence coefficient, deflection relative to $x_{1(0)}$ of rth mass, of jth branch, due to a unit force at sth mass of kth branch, inches/pound force (meters/newton)
j	index denoting jth branch
k	index denoting kth branch

L overall length of main or 0th branch, inches (meters)

m mass per unit length, $\frac{\text{pounds-seconds}^2}{\text{inch}^2}$ $\left(\frac{\text{newtons-seconds}^2}{\text{meters}^2}\right)$

$m_{s(k)}$ sth mass of kth branch located at $x_{s(k)}$, $\frac{\text{pounds-seconds}^2}{\text{inch}}$ $\left(\frac{\text{newtons-seconds}^2}{\text{meter}}\right)$

M total mass, $\frac{\text{pounds-seconds}^2}{\text{inch}}$ $\left(\frac{\text{newtons-seconds}^2}{\text{meter}}\right)$

n index denoting total number of lumped masses in a system

p index, corresponds to pth natural mode

q index, corresponds to qth natural mode

t time, sec

u displacement from unstrained position, function of x and t, inches (meters)

$v(k)$ index denoting total number lumped masses on kth branch

x longitudinal coordinate, inches (meters)

$x_{r(j)}, x_{s(k)}$ distance of r(j)th, s(k)th lumped mass from origin, inches (meters)

η exponent for parameter study

λ eigenvalue

ξ longitudinal coordinate, inches (meters)

$\varphi_{r(j)}, \varphi_{s(k)}$ displacement amplitude, function of x, denotes deflection from unstrained position of r(j)th, s(k)th discrete mass, inches (meters)

ω circular frequency of simple harmonic vibration, radians/second

Subscripts:

a	ath row of a matrix
b	bth column of a matrix
r(j)	rth mass of jth branch
s(k)	sth mass of kth branch
max	maximum
ref	reference

Matrix notation:

$\begin{bmatrix} \ddots \end{bmatrix}$	diagonal matrix
$\begin{bmatrix} \end{bmatrix}$	square or rectangular matrix
$\begin{bmatrix} \end{bmatrix}^T$	transpose of matrix
$\begin{bmatrix} \cdots \end{bmatrix}$	row matrix
$\begin{Bmatrix} \\ \\ \end{Bmatrix}$	column matrix
$\begin{bmatrix} 1 & & \\ & \ddots & \\ & & 1 \end{bmatrix}$	identity matrix
$\begin{bmatrix} 1 & \cdots & 1 \\ \vdots & & \vdots \\ 1 & \cdots & 1 \end{bmatrix}$	square matrix of all unit elements
$\begin{bmatrix} 1 & \cdots & 1 \end{bmatrix}$	row matrix of all unit elements
$\begin{Bmatrix} 1 \\ \vdots \\ 1 \end{Bmatrix}$	column matrix of all unit elements

ANALYSIS

A lumped mass analogy of a beam is developed. This analogy is then extended to obtain a lumped mass representation of a general unconstrained multibranch beam. Through an influence coefficient approach, the longitudinal equations of motion for the lumped mass system are derived in terms of one-dimensional beam theory and reduced to a matrix eigenvalue problem which determines the natural frequencies and the associated modal vectors. A procedure for computing the influence coefficients is given, the orthogonal properties of the modal vectors are demonstrated, and an iterative method is presented for solving the eigenvalue problem. Since these equations are based on one-dimensional beam theory, they should be applied with reservation to structures which depart from this concept (e.g., thin-wall cylindrical shells of large diameter, shells containing a sloshing fluid, etc.).

Derivation of the Lumped Mass Equations for a Single Beam

The so-called "lumped mass" analogy in which a structure is represented as a series of lumped masses connected by massless springs offers an effective simple approach to vibration analyses. The transition from a continuous system to a lumped system, however, has generally been somewhat of an arbitrary process which depended on the judgment of the analyst. A formal derivation of the lumped mass approach is obtained by the direct collocation method as shown herein. This process involves satisfying the integral equations of motion at a finite number of selected points.

Consider a general nonuniform beam (sketch 1) which is fixed at an arbitrary point x_f with a concentrated axial unit load applied at $X = \xi$. The resulting deflection at any point x due to the unit load at ξ is designated as the Green's function or influence function $G(x, \xi)$.

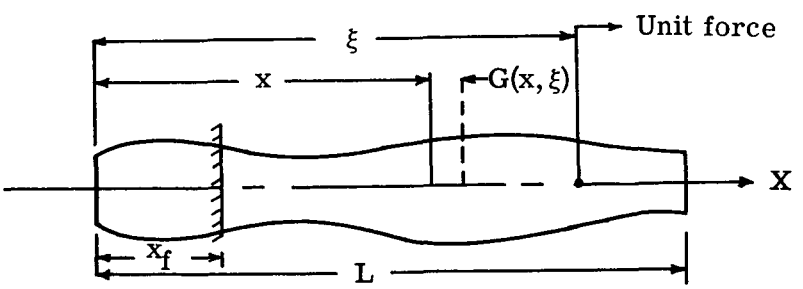

Sketch 1

By utilizing this influence function, the deflection $u(x,t)$ at any point x due to a distributed axial force $F(\xi,t)$, which includes inertial forces, is given by superposition as

$$u(x,t) = \int_0^L G(x, \xi)\ F(\xi,t)\ d\xi \qquad (1)$$

If the fixity constraint at x_f is released and the beam is allowed to translate as a free body, equation (1) becomes

$$u(x,t) = u(x_f,t) + \int_0^L G(x,\xi)\, F(\xi,t)\, d\xi \tag{2}$$

where $u(x_f,t)$ is the rigid body displacement of the influence function reference point x_f. Assume that the unconstrained or free-free beam vibrates in simple harmonic motion of frequency ω and amplitude $\varphi(x)$; then,

$$u(x,t) = \varphi(x)\, e^{i\omega t} \tag{3}$$

where $i = \sqrt{-1}$. In the absence of external forces the axial force is caused only by the inertia loading of the distributed mass $m(x)$ and is given as

$$F(x,t) = -m(x)\, \ddot{u}(x,t) = \omega^2 m(x)\, \varphi(x)\, e^{i\omega t} \tag{4}$$

where a dot denotes differentiation with respect to time. Substituting equations (3) and (4) into equation (2) and canceling $e^{i\omega t}$ gives

$$\varphi(x) = \varphi(x_f) + \omega^2 \int_0^L G(x,\xi)\, m(\xi)\, \varphi(\xi)\, d\xi \tag{5}$$

The beam length from $x = 0$ to $x = L$ is divided into v intervals (sketch 2) which are arbitrarily spaced except that an interval marker is assumed to coincide with any discontinuity in axial stiffness. The interval boundaries are denoted by x_s where $s = 1$ to $v + 1$.

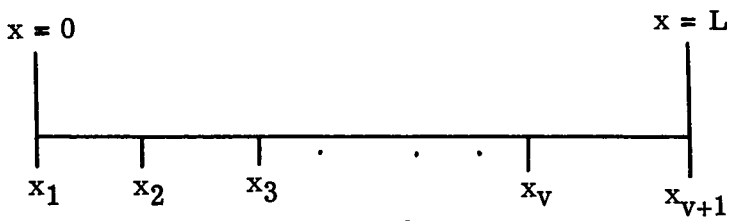

Sketch 2

By introducing the function $H(x,\xi) = G(x,\xi)\, \varphi(\xi)$, equation (5) can be written as

$$\varphi(x) = \varphi(x_f) + \omega^2 \sum_{s=1}^{v} \int_{x_s}^{x_{s+1}} H(x,\xi)\, m(\xi)\, d\xi \tag{6}$$

The structure is continuous in the neighborhood of ξ_s so that the function $H(x,\xi)$ can be expanded into a Taylor series about ξ_s, where $x_s < \xi_s < x_{s+1}$, to give

$$H(x,\xi) = H(x,\xi_s) + H'(x,\xi_s)(\xi - \xi_s) + O\Delta\xi_s^2 \tag{7}$$

where the prime denotes $d/d\xi$ and $O\Delta\xi_s^2$ denotes terms of order $(\xi - \xi_s)^2$ and higher. Neglecting higher order terms and substituting equation (7) into equation (6) yields the approximate relationship

$$\varphi(x) = \varphi(x_f) + \omega^2 \sum_{s=1}^{v} \left[H(x,\xi_s) \int_{x_s}^{x_{s+1}} m(\xi)\, d\xi + H'(x,\xi_s) \int_{x_s}^{x_{s+1}} m(\xi)(\xi - \xi_s)\, d\xi \right] \tag{8}$$

In equation (8) if ξ_s is chosen to be the mass center of gravity between x_s and x_{s+1}, then the second integral vanishes identically. Therefore, by defining

$$\xi_s = \frac{\int_{x_s}^{x_{s+1}} m(\xi)\xi\, d\xi}{\int_{x_s}^{x_{s+1}} m(\xi)\, d\xi} \tag{9}$$

and

$$m_s = \int_{x_s}^{x_{s+1}} m(\xi)\, d\xi \tag{10}$$

equation (8) becomes

$$\varphi(x) = \varphi(x_f) + \omega^2 \sum_{s=1}^{v} G(x,\xi_s) m_s \varphi_s \tag{11}$$

where $\varphi_s = \varphi(\xi_s)$.

The vanishing of the second integral in equation (8) when ξ_s is chosen to be the interval center of gravity (c.g.) suggests that this is an optimum location of the point mass to minimize the error bounds (i.e., the maximum possible error involved in replacing the continuous system by the lumped mass system). Further discussion of these approximation errors is presented in a subsequent section.

For convenience, $x_f = \xi_1$ is chosen to be the reference point for the influence function $G(x,\xi)$. Equation (11) for $x = \xi_r$, where $r = 1$ to v, yields a set of equations which can be conveniently written in matrix notation as

$$\{\varphi_r\} = \varphi_1\{1\} + \omega^2 [G_{r,s}][m_s]\{\varphi_s\} \tag{12}$$

where $G_{r,s} = G(\xi_r, \xi_s)$ and r,s = 1 to v.

It is more convenient and equally correct to write equation (12) as

$$\{\varphi_r\} = \varphi_1\{1\} + \omega^2[G_{r,s}][m_r]\{\varphi_r\} \tag{13}$$

where r,s = 1 to v.

Derivation of the Lumped Mass Equations for a Multibranch Beam

The lumped mass approach established for a single beam is extended herein to derive similar equations of motion for a class of multibranch beams; this class consists of a main beam with subsidiary beams attached along its axis like a tree trunk and its branches. Further, the subsidiary or branch beams are parallel to the main branch.

For branch identification purposes, the main branch is denoted as the 0th branch; all subbranches are denoted by the mass on the 0th branch to which they are attached.

The lumped masses of each branch are numbered consecutively from 1. The masses of the various branches are then distinguished from each other by a branch index which appears in parentheses after the mass number. The same mass-number—branch-number index system is also used for the x-locations of the respective masses.

Consider, for a moment, the main branch of a general multibranch beam. This branch can be divided into "v(0)" panels or intervals of arbitrary length as shown by the dashed line in sketch 3.

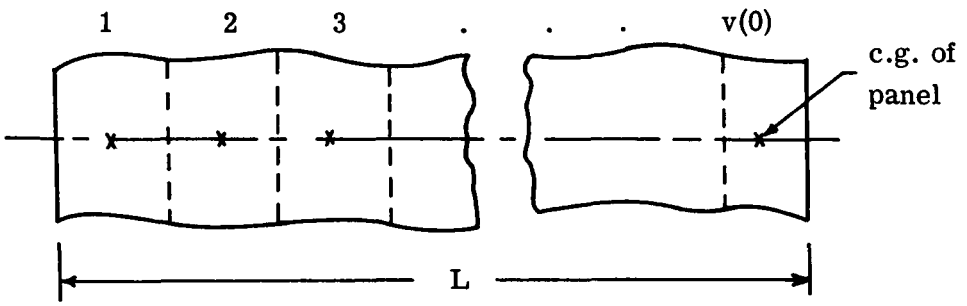

Sketch 3

The total weight of each panel can then be concentrated in the form of a lumped mass at its center of gravity $x_{r(0)}$, where r = 1 to v(0). (See sketch 4.) To be consistent with the notation introduced, it is necessary that each subbranch attach to a mass on the main branch.

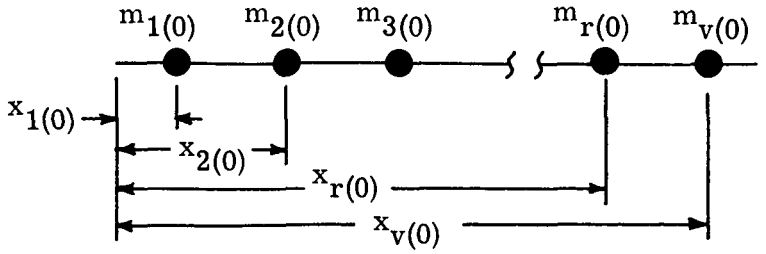

Sketch 4

Then as shown in sketch 5, any subbranch can be lumped and attached to the appropriate mass on the main branch.

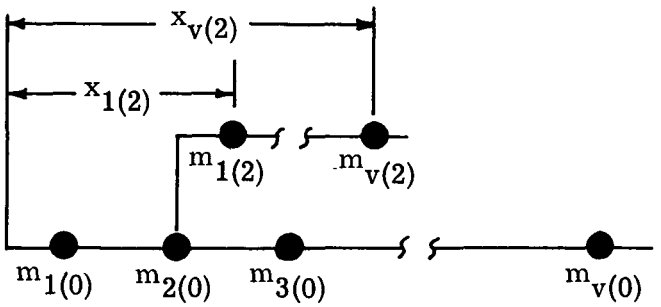

Sketch 5

Let $G_{r(j),s(k)}$ define the deflection, relative to $x_{1(0)}$, at $x = x_{r(j)}$ due to a unit force at $x = x_{s(k)}$. The total deflection at station $x_{r(j)}$ is then given by superposition as

$$u_{r(j)} = u_{1(0)} + \sum_{k=0}^{v(0)} \sum_{s=1}^{v(k)} G_{r(j),s(k)} F_{s(k)} \tag{14}$$

where $u_{1(0)}$ is the rigid body translation of the reference point $x_{1(0)}$ and $F_{s(k)}$ is the axial inertia force at $x = x_{s(k)}$. The right-hand summation of equation (14) is over the total number of masses of a given branch and the left-hand summation is over the total number of branches.

Equation (14) is formulated as though a branch is located at every mass on the 0th branch. The equation holds for fewer branches, however, if the subscripts j and k only assume the values corresponding to branch locations (in addition to 0 for the main branch). For example, if branches were located at $x_{1(0)}$, $x_{5(0)}$, and $x_{7(0)}$, then

$$j,k = 0, 1, 5, 7$$

The subscripts j and k always begin with 0, and for systems consisting only of the main branch they only assume the value of 0.

If j = 0 to v(0) and equations (3) and (4) are utilized, equation (14) yields a set of equations which can be written in the following matrix form:

$$\left\{\varphi_{r(j)}\right\} = \varphi_{1(0)}\left\{1\right\} + \omega^2\left[G_{r(j),s(k)}\right]\left[m_{s(k)}\right]\left\{\varphi_{s(k)}\right\} \tag{15}$$

where

$$r = 1 \text{ to } v(j)$$

$$s = 1 \text{ to } v(k)$$

$$j,k = 0 \text{ to } v(0)$$

$$\left\{\varphi_{r(j)}\right\} = \begin{Bmatrix} \varphi_{r(0)} \\ \varphi_{r(1)} \\ \varphi_{r(2)} \\ \vdots \end{Bmatrix}$$

$$\left[G_{r(j),s(k)}\right] = \begin{array}{c} \\ j \downarrow \\ r \end{array} \begin{array}{c} k \longrightarrow \\ s \longrightarrow \end{array} \begin{bmatrix} G_{r(0),s(0)} & G_{r(0),s(1)} & G_{r(0),s(2)} & \cdots \\ G_{r(1),s(0)} & G_{r(1),s(1)} & G_{r(1),s(2)} & \cdots \\ G_{r(2),s(0)} & G_{r(2),s(1)} & G_{r(2),s(2)} & \cdots \\ \vdots & \vdots & \vdots & \ddots \end{bmatrix}$$

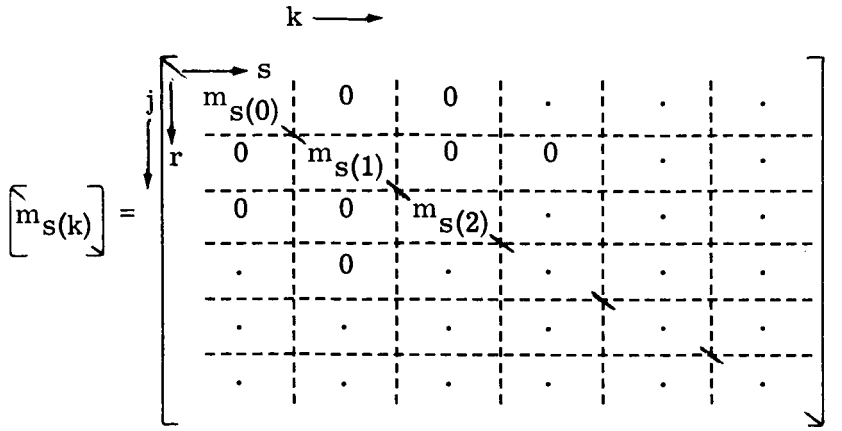

Each of the dotted-line compartments represents a partitioned submatrix. As for equation (12), it is correct and useful to write equation (15) as

$$\left\{\varphi_{r(j)}\right\} = \varphi_{1(0)}\left\{1\right\} + \omega^2\left[G_{r(j),s(k)}\right]\left[m_{r(j)}\right]\left\{\varphi_{r(j)}\right\} \tag{16}$$

Equations (14), (15), and (16) are then respectively analogous to equations (11), (12), and (13) which were previously derived.

Since the beam is considered to be free or unconstrained, longitudinal equilibrium requires that

$$\sum_{j=0}^{v(0)} \sum_{r=1}^{v(j)} F_{r(j)} = 0 \tag{17}$$

Again, by utilizing equations (3) and (4) equation (17) leads to

$$\sum_{j=0}^{v(0)} \sum_{r=1}^{v(j)} \varphi_{r(j)}\, m_{r(j)} = 0$$

or in matrix form to

$$\left[1\right]\left[m_{r(j)}\right]\left\{\varphi_{r(j)}\right\} = 0 \tag{18}$$

Premultiplying equation (16) by $\left[1\right]\left[m_{r(j)}\right]$, utilizing equation (18), and solving for $\varphi_{1(0)}$ gives

$$\varphi_{1(0)} = \frac{-\omega^2}{M}\left[1\right]\left[m_{r(j)}\right]\left[G_{r(j),s(k)}\right]\left[m_{r(j)}\right]\left\{\varphi_{r(j)}\right\} \tag{19}$$

where

$$M = \left[1\right]\left[m_{r(j)}\right]\left[1\right]$$

is the total mass of the system. Substituting equation (19) into equation (16) gives

$$\left[B_{r(j),s(k)}\right]\left[G_{r(j),s(k)}\right]\left[m_{r(j)}\right]\left\{\varphi_{r(j)}\right\} = \frac{1}{\omega^2}\left\{\varphi_{r(j)}\right\} \tag{20}$$

where

$$\left[B_{r(j),s(k)}\right] = \left[\left[1\right] - \left[1\right]\left[m_{r(j)}/M\right]\right]$$

The index notation of equation (20) has utility only in the derivation and interpretation of the numbers which form the matrix arrays. Therefore, to simplify the notation the following matrices are redefined and used interchangeably:

$$\left[B\right] = \left[B_{a,b}\right] = \left[B_{r(j),s(k)}\right]$$

$$\left[G\right] = \left[G_{a,b}\right] = \left[G_{r(j),s(k)}\right]$$

$$\left[m\right] = \left[m_a\right] = \left[m_{r(j)}\right]$$

$$\left\{\varphi\right\} = \left\{\varphi_a\right\} = \left\{\varphi_{r(j)}\right\}$$

where

$a,b = 1$ to n

$r = 1$ to $v(j)$

$s = 1$ to $v(k)$

$j,k = 0$ to $v(0)$

and the subscript n represents the total number of lumped masses comprising the system.

Equation (20) can then be written more compactly as

$$\left[D_{a,b}\right]\left\{\varphi_a\right\} = \lambda\left\{\varphi_a\right\} \tag{21}$$

where

$$a,b = 1 \text{ to } n$$

$$\left[D_{a,b}\right] = \left[B_{a,b}\right]\left[G_{a,b}\right]\left[m_a\right]$$

and

$$\lambda = \frac{1}{\omega^2}$$

Equation (21) is the familiar form for a matrix eigenvalue problem and can be solved by a number of classical procedures. One of these procedures (an iterative solution involving orthogonality sweeping for determining modes higher than the fundamental) is presented subsequently.

Calculation of Influence Coefficients

Consider a beam fixed at station $x_{1(0)}$ with a unit load applied in the positive x-direction at station $x_{s(k)}$ as shown in sketch 6.

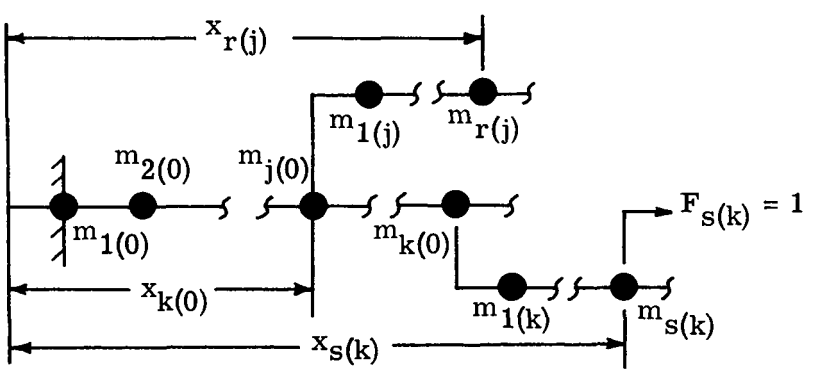

Sketch 6

The deflection at any point $x_{r(j)}$ is then defined as an influence coefficient. These deflections or influence coefficients $G_{r(j),s(k)}$ are derived for all combinations of $j \leq k$ through the use of elementary one-dimensional beam theory, as follows:

For $j = k = 0$,

$$G_{r(0),s(0)} = \int_{x_{1(0)}}^{x_{r(0)}} \frac{dx}{A(0)\,E(0)} \qquad (r \leqq s) \qquad (22)$$

For $j = 0$ and $k \neq 0$,

$$G_{r(0),s(k)} = \int_{x_{1(0)}}^{x_{r(0)}} \frac{dx}{A(0)\,E(0)} \qquad (r \leqq k) \qquad (23)$$

$$G_{r(0),s(k)} = \int_{x_{1(0)}}^{x_{k(0)}} \frac{dx}{A(0)\,E(0)} \qquad (r > k) \qquad (24)$$

For $j,k \neq 0$,

$$G_{r(j),s(k)} = \int_{x_{1(0)}}^{x_{j(0)}} \frac{dx}{A(0)\,E(0)} \qquad (j < k) \qquad (25)$$

$$G_{r(j),s(k)} = \int_{x_{1(0)}}^{x_{j(0)}} \frac{dx}{A(0)\,E(0)} + \left| \int_{x_{j(0)}}^{x_{r(j)}} \frac{dx}{A(j)\,E(j)} \right| \qquad (26)$$

$(j = k \quad \text{and} \quad r \leqq s)$

The absolute value of the integral in equation (26) allows for the possibility of a branch in either the positive or negative x-direction.

All values of the influence coefficients for $j > k$ can be determined from Maxwell's reciprocal theorem; thus,

$$G_{r(j),s(k)} = G_{s(k),r(j)} \qquad (27)$$

The $1/AE$ function in the $G_{r(j),s(k)}$ integral is generally a highly discontinuous function and, therefore, a numerical form of integration is expedient. A simple quadrature numerical integration will give excellent results and yields the exact answer provided that the $1/AE$ curve is a straight line between intermediate integration points. For a curved line, the intermediate integration points should be generously chosen so that the curve can be approximated as a straight line between them.

Application of the Method to Torsional Vibrations

The Saint-Venant torsion theory for prismatical bars leads to the following classical equation of motion for torsional vibrations:

$$\frac{\partial}{\partial x}\left(C\,\frac{\partial \theta}{\partial x}\right) = I\,\frac{\partial^2 \theta}{\partial t^2} \tag{28}$$

where

$C = C(x)$ torsional rigidity (ref. 9)

$I = I(x)$ polar mass moment of inertia per unit length

$\theta = \theta(x,t)$ cross-section rotation

For a circular cross section the torsional rigidity is

$$C = JG \tag{29}$$

where J is the polar moment of inertia of the cross section and G is the shear modulus. Equation (28), for bodies of revolution, thus becomes

$$\frac{\partial}{\partial x}\left(JG\,\frac{\partial \theta}{\partial x}\right) = I\,\frac{\partial^2 \theta}{\partial t^2} \tag{30}$$

The similar one-dimensional equation of motion for longitudinal vibrations on which the derivations of foregoing sections are founded is

$$\frac{\partial}{\partial x}\left(AE\,\frac{\partial u}{\partial x}\right) = m\,\frac{\partial^2 u}{\partial t^2} \tag{31}$$

where

$A = A(x)$ cross-sectional area

E modulus of elasticity

$m = m(x)$ mass per unit length

$u = u(x,t)$ cross-section displacement

If equation (28) (or eq. (30)) is compared with equation (31), it is seen that C (or JG) is analogous to AE, I is analogous to m, and θ is analogous to u. Therefore, by replacing AE, m, and u with C, I, and θ, respectively, all the previously derived equations for the longitudinal vibration of beams can be applied directly to torsional analyses of structures whose equation of motion is compatible with equation (28). This compatibility is only satisfied when the elastic axes of all branches are everywhere concentric.

Derivation of Orthogonality Relationships

Several of the classical iteration techniques for solving equation (21) depend upon orthogonality relationships for obtaining modes higher than the fundamental. These relationships are derived herein.

From equation (16), the equation for the pth natural mode can be written as

$$\{\varphi(p)\} = \varphi_1(p)\{1\} + \omega^2(p)[G][m]\{\varphi(p)\} \tag{32}$$

where $\varphi_1(p) = \varphi_{1(0)}(p)$. Premultiplying equation (32) by $\lfloor\varphi(q)\rfloor[m]$, where $\lfloor\varphi(q)\rfloor$ is the qth natural mode, gives

$$\lfloor\varphi(q)\rfloor[m]\{\varphi(p)\} = \lfloor\varphi(q)\rfloor[m]\{1\}\,\varphi_1(p) + \omega^2(p)\lfloor\varphi(q)\rfloor[m][G][m]\{\varphi(p)\} \tag{33}$$

Proceeding in a similar manner for the qth mode gives

$$\lfloor\varphi(p)\rfloor[m]\{\varphi(q)\} = \lfloor\varphi(p)\rfloor[m]\{1\}\,\varphi_1(q) + \omega^2(q)\lfloor\varphi(p)\rfloor[m][G][m]\{\varphi(q)\} \tag{34}$$

The transposition of equation (18) gives

$$\lfloor\varphi(q)\rfloor[m]\{1\} = \lfloor\varphi(p)\rfloor[m]\{1\} = 0 \tag{35}$$

Also, since $[G]$ and $[m]$ are symmetrical,

$$\lfloor\varphi(q)\rfloor[m][G][m]\{\varphi(p)\} = \lfloor\varphi(p)\rfloor[m][G][m]\{\varphi(q)\} \tag{36a}$$

and

$$\lfloor\varphi(q)\rfloor[m]\{\varphi(p)\} = \lfloor\varphi(p)\rfloor[m]\{\varphi(q)\} \tag{36b}$$

Therefore, subtracting equation (34) from equation (33) and utilizing equations (35) and (36) gives

$$\left(\omega^2(p) - \omega^2(q)\right)\lfloor\varphi(q)\rfloor[m][G][m]\{\varphi(p)\} = 0 \tag{37}$$

Then from equation (37) for $p \neq q$

$$\lfloor\varphi(q)\rfloor[m][G][m]\{\varphi(p)\} = 0 \tag{38a}$$

Substituting equations (35) and (38a) into equation (33) gives

$$\left[\varphi(q)\right]\left[m\right]\left\{\varphi(p)\right\} = 0 \tag{38b}$$

for $p \neq q$.

Equations (38) are then two valid orthogonality relationships. Equation (38b) is generally preferred, however, because of its simplicity.

Solutions to Eigenvalue Problem

It is beyond the scope of this paper to enumerate the iterative procedures for solving eigenvalue problems and to discuss the advantages of each. The methods can generally be categorized into two basic types: those which replace a trial vector with an improved trial vector, and those which replace a square matrix with an improved square matrix. A method of each type is discussed briefly herein.

Iteration and sweeping.- A classical method for solving eigenvalue problems involves the replacement of a trial vector by an improved vector obtained by multiplying the trial vector by the coefficient matrix. The method is classical and is documented in numerous works (e.g., ref. 10). Applying this process to equation (21), however, gives only the fundamental mode.

Equation (21) can be modified by any one of several different procedures to determine higher modes. One particular method which has proved very satisfactory is outlined in reference 11. By utilizing the orthogonality relationship (eq. (38b)), the higher modes can be determined by the iteration of the following modified matrix equation:

$$\left[D(p)\right]\left\{\varphi\right\} = \lambda\left\{\varphi\right\} \qquad (p = 2, 3, \ldots, n-1) \tag{39}$$

where

$$\lambda = \frac{1}{\omega^2}$$

$$\left[D(p)\right] = \left[D\right]\left[S(p)\right]$$

$\left[D\right]$ is defined by equation (21)

$$\left[S(2)\right] = \left[\left[1\right] - \frac{\left\{\varphi_a(1)\right\}\left[\varphi_a(1)\right]\left[m_a\right]}{\left[\varphi_a(1)\right]\left[m_a\right]\left\{\varphi_a(1)\right\}}\right]$$

and

$$\left[S(p)\right] = \left[\left[S(p-1)\right] - \frac{\left\{\varphi_a(p-1)\right\}\left[\varphi_a(p-1)\right]\left[m_a\right]}{\left[\varphi_a(p-1)\right]\left[m_a\right]\left\{\varphi_a(p-1)\right\}}\right]$$

$(p = 3, 4, 5, \ldots, n)$

The $[S(p)]$ matrix is a so-called sweeping matrix which removes the components of all modes below the pth mode from the trial iteration vector $\{\varphi_a\}$. This method is suitable for desk calculator or digital computer solution.

The characteristic polynomial of equation (39) clearly is of order "n"; therefore, the system has "n" eigenvalues (λ's). Only $n - 1$ of these eigenvalues and modes can be obtained by iteration. The remaining mode is spurious and corresponds to a zero eigenvalue (λ). The existence of this spurious mode can be proved as follows:

It is noted in equation (21) that

$$[D] = [B][G][m] \tag{40}$$

Since $[G]$ is the influence coefficient matrix for a beam fixed at the first mass, the first row and first column of $[G]$ are null, and $[G]$ is, therefore, singular. It then follows from the theory of determinants (ref. 12, p. 25) that $[D]$ is also singular – that is,

$$\left|[D]\right| = 0 \tag{41}$$

It can be further concluded from the theory of determinants (ref. 12, pp. 68-69) that the singularity of $[D]$ necessitates a zero eigenvalue (λ) of equation (21).

The mode corresponding to this zero eigenvalue must satisfy equation (21) for $\lambda = 0$. Thus,

$$[D]\{\varphi\} = 0 \tag{42}$$

The singularity of $[D]$ is a necessary and sufficient condition to guarantee a nontrivial solution to equation (42) (ref. 13). This nontrivial solution has no physical significance and can be shown by substitution to be

$$\{\varphi\} = \begin{Bmatrix} 1 \\ 0 \\ 0 \\ \cdot \\ \cdot \\ \cdot \\ 0 \end{Bmatrix} \tag{43}$$

From physical considerations there are $n - 1$ elastic modes and one rigid body (zero frequency) mode associated with the lumped mass system which led to equation (21). The transformation resulting from equation (19) eliminated the rigid body mode and replaced it by the aforementioned spurious mode. Iteration of equation (21) thus only yields the $n - 1$ dominant elastic modes.

Matrix diagonalization.- The computer age has revived interest in methods for solving characteristic value problems in which the coefficient matrix is brought to diagonal or nearly diagonal form by a sequence of orthogonal transformations. Among these are many variations of an old procedure formulated by Jacobi in which the matrix is diagonalized; this matrix diagonalization leads to solution for all modes and frequencies simultaneously. In a recent innovation by Givens (ref. 10, pp. 336-340) the original matrix is transformed to tridiagonal form and the eigenvalues are then computed from a Sturm sequence.

All such methods, however, require the eigenvalue problem to be in the following form:

$$[E]\{\varphi\} = \lambda\{\varphi\} \tag{44}$$

where $[E]$ is a real symmetric matrix and λ is the eigenvalue. Equation (21) can be put in the form of equation (44) by the following procedure.

A sweeping matrix similar to that of equation (39) is utilized to remove the rigid body mode $\{\phi(0)\} = \{1\}$ from the trial vector. This sweeping matrix is

$$[S(1)] = \left[[1] - \frac{1}{M}[1][m]\right] = [m]^{-1}[B]^T[m] \tag{45}$$

where $[B]^T$ is the transpose of the $[B]$ matrix of equation (20). Since the rigid body mode has already been eliminated, this step is redundant. It does, however, lead to the desired symmetrical form.

It can be seen from equation (18) that $[S(1)]$ possesses the property

$$[S(1)]\{\varphi(p)\} = \{\varphi(p)\} \qquad (p = 1, 2, 3, \ldots, n - 1) \tag{46}$$

Substituting equations (45) and (46) into equation (21) gives

$$[B][G][B]^T[m]\{\varphi\} = \frac{1}{\omega^2}\{\varphi\} \tag{47}$$

Then, introducing the change in variables

$$\{y\} = [m]^{1/2}\{\varphi\} \tag{48}$$

into equation (47) leads to

$$[m]^{1/2}[B][G][B]^T[m]^{1/2}\{y\} = \frac{1}{\omega^2}\{y\} \tag{49}$$

Equation (49) is then in the form of equation (44) where

$$[E] = [m]^{1/2}[B][G][B]^T[m]^{1/2}$$

$$\lambda = \frac{1}{\omega^2}$$

After solving equation (49) for $\{y\}$, the original modal matrix is obtained from equation (48) as

$$\{\varphi\} = [m]^{-1/2}\{y\} \tag{50}$$

The system given by equation (47) also has a spurious mode which corresponds to a zero eigenvalue (λ). The proof is similar to the one given in the preceding section. The spurious modal vector in this case, however, turns out to be identical to the rigid body mode in contrast to the form of equation (43). This identity can be shown as follows:

From equation (45), equation (47) can be written as

$$[B][G][m][S(1)]\{\varphi\} = \lambda\{\varphi\}$$

where $\lambda = \frac{1}{\omega^2}$. If $\lambda = 0$, the spurious mode must satisfy

$$[B][G][m][S(1)]\{\varphi\} = 0$$

This equation is obviously satisfied by the rigid body mode $\{\varphi\} = \{1\}$ since

$$[S(1)]\{1\} = 0$$

NUMERICAL EXAMPLES

Idealized Beam

For the purpose of showing the operations of the matrices derived in the foregoing section, the idealized beam shown in sketch 7 is considered. This example consists of a solid uniform beam attached to the inside of a uniform cylindrical shell by a massless, infinitely rigid point attachment which coincides with the shell center of gravity.

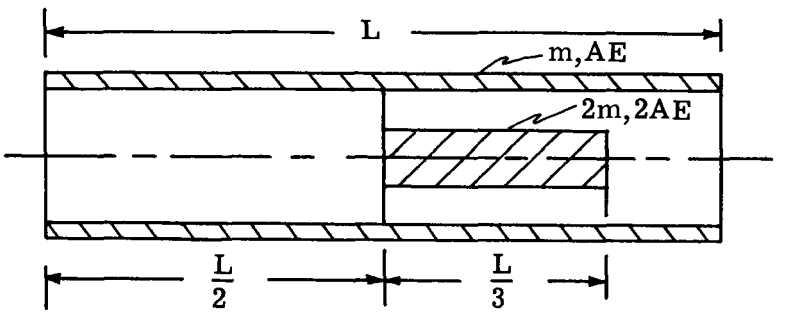

Sketch 7

For simplicity of illustration, the cylindrical shell is represented by three equal panels and the solid inner beam by one panel. The total mass of each panel can be considered concentrated at the panel center of gravity as shown by the analogous beam in sketch 8.

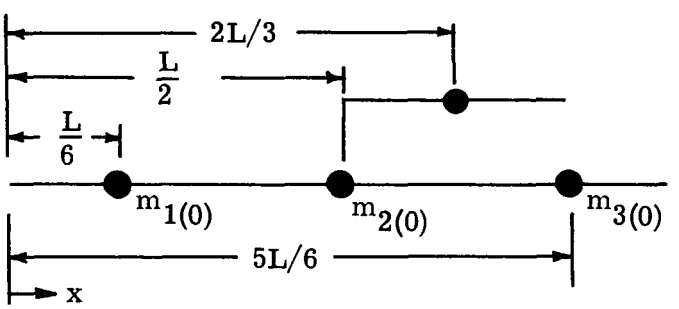

Sketch 8

Assume that the cross-sectional properties of the cylindrical shell are $m(x)$ and $A(x)\,E(x)$ and those of the solid inner beam are $2m(x)$ and $2A(x)\,E(x)$. The matrices used to formulate equation (21) are then

$$[m] = \frac{mL}{3}\left[\begin{array}{ccc:c} 1 & 0 & 0 & 0 \\ 0 & 1 & 0 & 0 \\ 0 & 0 & 1 & 0 \\ \hdashline 0 & 0 & 0 & 2 \end{array}\right] \tag{51}$$

$$[G] = \frac{L}{12AE}\left[\begin{array}{ccc:c} 0 & 0 & 0 & 0 \\ 0 & 4 & 4 & 4 \\ 0 & 4 & 8 & 4 \\ \hdashline 0 & 4 & 4 & 5 \end{array}\right] \tag{52}$$

$$[B] = \begin{bmatrix} 1 & 0 & 0 & 0 \\ 0 & 1 & 0 & 0 \\ 0 & 0 & 1 & 0 \\ 0 & 0 & 0 & 1 \end{bmatrix} - \frac{1}{5}\begin{bmatrix} 1 & 1 & 1 & 1 \\ 1 & 1 & 1 & 1 \\ 1 & 1 & 1 & 1 \\ 1 & 1 & 1 & 1 \end{bmatrix}\begin{bmatrix} 1 & 0 & 0 & 0 \\ 0 & 1 & 0 & 0 \\ 0 & 0 & 1 & 0 \\ 0 & 0 & 0 & 2 \end{bmatrix} = \frac{1}{5}\begin{bmatrix} 4 & -1 & -1 & -2 \\ -1 & 4 & -1 & -2 \\ -1 & -1 & 4 & -2 \\ -1 & -1 & -1 & 3 \end{bmatrix} \tag{53}$$

where the 0th branch parameters are indicated by the upper left-hand partition matrices.

Substituting equations (51), (52), and (53) into equation (21) gives

$$\frac{mL^2}{90AE}\begin{bmatrix} 0 & -8 & -10 & -18 \\ 0 & 2 & 0 & 2 \\ 0 & 2 & 10 & 2 \\ 0 & 2 & 0 & 7 \end{bmatrix}\left\{\varphi_a\right\} = \frac{1}{\omega^2}\left\{\varphi_a\right\} \tag{54}$$

After iteration of equation (54) the following solutions are obtained for the fundamental flexible mode:

$$\left\{\varphi_a(1)\right\} = \begin{Bmatrix} -1 \\ 0 \\ 1 \\ 0 \end{Bmatrix} \tag{55a}$$

$$\omega(1) = \frac{3}{L}\sqrt{\frac{AE}{m}} \tag{55b}$$

Substituting equations (55) into the expression for $[S(2)]$ of equation (39) gives

$$\left[S(2)\right] = \begin{bmatrix} 1 & 0 & 0 & 0 \\ 0 & 1 & 0 & 0 \\ 0 & 0 & 1 & 0 \\ 0 & 0 & 0 & 1 \end{bmatrix} - \frac{\begin{Bmatrix} -1 \\ 0 \\ 1 \\ 0 \end{Bmatrix} \begin{bmatrix} -1 & 0 & 1 & 0 \end{bmatrix} \begin{bmatrix} 1 & 0 & 0 & 0 \\ 0 & 1 & 0 & 0 \\ 0 & 0 & 1 & 0 \\ 0 & 0 & 0 & 2 \end{bmatrix}}{\begin{bmatrix} -1 & 0 & 1 & 0 \end{bmatrix} \begin{bmatrix} 1 & 0 & 0 & 0 \\ 0 & 1 & 0 & 0 \\ 0 & 0 & 1 & 0 \\ 0 & 0 & 0 & 2 \end{bmatrix} \begin{Bmatrix} -1 \\ 0 \\ 1 \\ 0 \end{Bmatrix}}$$

$$\left[S(2)\right] = \frac{1}{2}\begin{bmatrix} 1 & 0 & 1 & 0 \\ 0 & 2 & 0 & 0 \\ 1 & 0 & 1 & 0 \\ 0 & 0 & 0 & 2 \end{bmatrix} \tag{56}$$

Substitution of equation (56) into the expression for $\left[D(p)\right]$ of equation (39) gives

$$\left[D(2)\right] = \frac{mL^2}{180AE}\begin{bmatrix} 0 & -8 & -10 & -18 \\ 0 & 2 & 0 & 2 \\ 0 & 2 & 10 & 2 \\ 0 & 2 & 0 & 7 \end{bmatrix}\begin{bmatrix} 1 & 0 & 1 & 0 \\ 0 & 2 & 0 & 0 \\ 1 & 0 & 1 & 0 \\ 0 & 0 & 0 & 2 \end{bmatrix}$$

$$\left[D(2)\right] = \frac{mL^2}{90AE}\begin{bmatrix} -5 & -8 & -5 & -18 \\ 0 & 2 & 0 & 2 \\ 5 & 2 & 5 & 2 \\ 0 & 2 & 0 & 7 \end{bmatrix} \tag{57}$$

Substituting equation (57) into equation (39) gives

$$\frac{mL^2}{90AE}\begin{bmatrix} -5 & -8 & -5 & -18 \\ 0 & 2 & 0 & 2 \\ 5 & 2 & 5 & 2 \\ 0 & 2 & 0 & 7 \end{bmatrix}\left\{\varphi_a\right\} = \frac{1}{\omega^2}\left\{\varphi_a\right\} \tag{58}$$

After iteration of equation (58), the following solutions are obtained for the second flexible mode:

$$\left\{\varphi_a(2)\right\} = \begin{Bmatrix} -1.0000 \\ 0.2986 \\ -1.0000 \\ 0.8507 \end{Bmatrix} \tag{59a}$$

$$\omega(2) = \frac{3.42}{L}\sqrt{\frac{AE}{m}} \tag{59b}$$

In a similar manner, the solutions for the third flexible mode are determined to be

$$\left\{\varphi(3)\right\} = \begin{Bmatrix} -0.1489 \\ 1.0000 \\ -0.1489 \\ -0.3511 \end{Bmatrix} \tag{60a}$$

$$\omega(3) = \frac{8.33}{L}\sqrt{\frac{AE}{m}} \tag{60b}$$

A plot of the three flexible modes obtained in this example are shown in figure 1. It is interesting to note that even with the inclusion of branches, the number of nodal points corresponds to the flexible mode number (i.e., the first flexible mode has one node point, etc.).

Typical Launch Vehicle

To show the application of the matrix solution to a more realistic beam, a numerical example of an application to a solid-fuel booster system is presented. The vehicle parameters are typical of those of the Scout class. The payload parameters were selected for purposes of illustration and are not necessarily representative of an existing payload. The following assumptions are employed:

(1) The solid-fuel mass is considered to adhere to the sides of the vehicle along the length and has no motion relative to the vehicle.

(2) The contribution of the fuel stiffness to the vehicle axial stiffness is negligible.

(3) Damping is considered to be negligible.

(4) All deformations are one-dimensional and no consideration is given to bending or breathing effects of the cylindrical shell walls.

Figures 2 and 3 show the rocket-vehicle mass and axial-extensional-coefficient data, respectively, in a desirable form for the analyst. The data for these graphs are given in tables 1, 2, and 3. The analogous discrete mass system is shown in figure 4. The X origin was chosen to coincide with the first discrete mass rather than the end of the beam.

The first three normalized natural modes and their corresponding natural frequencies obtained from the iteration of equation (21) are shown in figure 5. Note the high amplitude of the payload motion in both the first and second modes of vibration as a result of the payload frequency being close to the lower frequencies of the vehicle. Such a design can cause extensive acceleration loading on sensitive payload instrumentation and should be avoided if at all possible.

In both the first and second modes, the vehicle is deflected in a manner analogous to that of the fundamental vehicle mode without the payload. The addition of the payload branch introduces a whole range of secondary coupled frequencies in which the payload oscillations are either in phase or out of phase with the vehicle oscillations.

DISCUSSION OF COMPUTATIONAL ACCURACY

The previously derived equations pertinent to the solution were programed for the IBM 7094 electronic data processing system. Some of the points of interest in the application of this method are discussed.

Choice of the Number of Lumped Masses

The matrix solution used herein is subject to an inherent error dependent upon the validity of an analogous lumped mass approximation to a continuous beam. To gain an insight into the accuracy of the matrix solution, comparisons were made between the theoretical and approximate results. As mentioned previously, closed form solutions for beams of arbitrarily varying cross sections are very difficult to obtain. Therefore, comparisons were limited to beams with uniform and exponentially varying cross sections. For the approximate solution the beams were divided into n equally spaced intervals with the lumped mass at the center of gravity. The exact solutions for these beams are derived in appendix A.

A standard accuracy parameter for frequency comparison is the percent error which is calculated as follows:

$$\text{Percent error} = \frac{\omega_{\text{exact}} - \omega_{\text{approx}}}{\omega_{\text{exact}}} \times 100$$

No convenient standard exists for mode comparison. For the purposes of this paper, a root-mean-square percent error (derived in appendix B) is used.

The percent error of the first five elastic modes as a function of the total number of lumped masses n is given in figures 6 and 7 for the frequencies and mode shapes, respectively. It can be seen in both figures that the cross-sectional exponential factor β has very little effect on the percent error, although the range of β considered produced

a wide variation in the distribution of cross-sectional area. These results indicate that both frequency and mode accuracy depend more on the number of masses than on the variation of cross-sectional area. As expected, the error curve asymptotically approaches zero for high values of n. In figure 7, considerable slope discontinuities are apparent in the curves toward the origin. These discontinuities, for a given mode, occur in the range where n is either 1 or 2 greater than the mode number. It is noted that in this range of n the addition of an extra mass may or may not be detrimental to the mode shape.

For most engineering applications, a 1-percent error limit is sufficient. Therefore, the 1-percent-error data for the first five modes from figures 6 and 7 are presented in figure 8. It can be seen that the solid line corresponding to the equation

$$n = 6i + 1$$

(where i is the highest mode to be determined) gives a "rule of thumb" for determining an adequate number of masses to obtain both the frequencies and the modes with this accuracy.

Advantages of Influence Coefficient Approach

In discrete element structural analysis, two approaches can be taken: the stiffness (spring) approach and the flexibility (influence coefficient) approach. The tendency is to adopt the stiffness approach without consideration of accuracy loss because the stiffness matrix is generally simpler to formulate than the flexibility matrix. The stiffness matrix approach, however, necessitates the formulation of the matrix eigenvalue problem such that the eigenvalue corresponding to the highest natural frequency is dominant.

The prime advantage of the flexibility approach is that the problem can be formulated so that the mode corresponding to the lowest natural frequency is dominant. It is generally accepted that the various means of solving eigenvalue problems lose accuracy when proceeding from the dominant mode to the subdominant modes. The magnitude of this accuracy degeneration varies somewhat with different methods of solution, but the author's experience and that of Batchelder and Wada (ref. 4) indicate that the error is dependent on the ratio of the dominant eigenvalue to the subdominant eigenvalue. Also, experience has shown that as this ratio becomes large, accuracy is lost in the subdominant modes.

A sizable spread between the dominant and subdominant frequencies can result from a large number of degrees of freedom and/or large variations in the stiffness or mass in different parts of the system. The stiffness matrix approach can lead to complete loss of accuracy in the lower modes, which are of prime interest; whereas, the flexibility matrix

approach only loses accuracy in the less important higher modes. This fact is simply illustrated by comparative solutions of the spring-mass system shown in sketch 9.

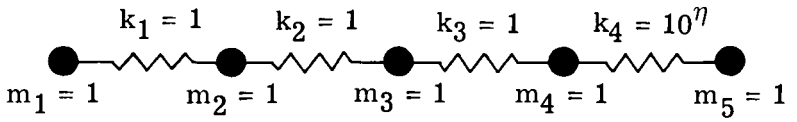

Sketch 9

From sketch 9 it can be seen that as the value of η becomes large, k_4 becomes large and the lower frequencies of the system approach those of the system shown in sketch 10(a). In addition, the value of k_3 becomes negligible in comparison with the value of k_4, and the highest frequency of the system approaches the frequency of the uncoupled two mass system shown in sketch 10(b). The frequencies of these two simple degenerate systems can be determined with high accuracy (by any method) and are, therefore, used as a reference for a subsequent comparative study.

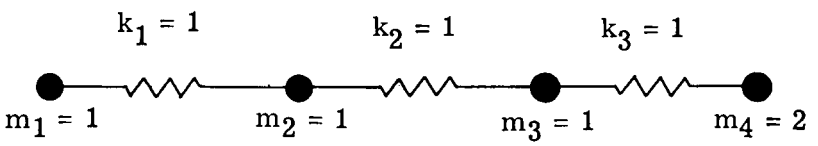

(a) First three modes.

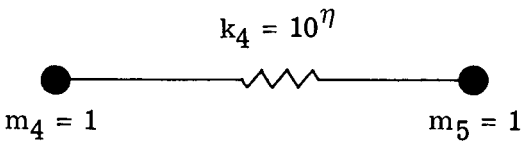

(b) Fourth mode.

Sketch 10

The natural frequencies were obtained as a function of increasing values of η for the system of sketch 9, by methods employing both the flexibility and stiffness matrices. The ratios of these frequencies to the aforementioned reference frequencies are given in table 4. If there were no loss of accuracy in computation, the ratios ω/ω_{ref} would approach unity as η becomes large. A departure from this pattern indicates loss of numerical accuracy in computation.

It can be seen that method I (Givens solution to stiffness matrix) gives good answers up to the point $\eta = 6$, which corresponds to an approximate ratio of 10^3 between the highest and the lowest mode frequencies. Beyond this point there is complete accuracy loss in all but the highest mode. Method II (iteration and sweeping solution to stiffness matrix) indicates similar accuracy loss in the lower modes; although, the drop-off is not as sharp

as in method I. Method III (iteration and sweeping solution to flexibility matrix) and method IV (Givens solution to flexibility matrix) give very similar answers and show no accuracy loss except in the highest mode. For low values of η all methods are seen to give nearly the same answers.

This example does not represent a real structure but it does point out the type of problems that can occur and have occurred to the author's knowledge in practical analyses of structures with widely varied mass and elastic properties. It also clearly demonstrates the increased lower mode computational accuracy obtained by the flexibility approach.

In many structural problems, the spread between the highest and lowest natural frequencies is small enough to yield satisfactory results by the stiffness matrix approach. There is always the element of doubt, however, and the analyst must be constantly aware of impending accuracy loss in the lower modes. The influence coefficient approach of this paper is thus advocated to yield confidence in the lower modes and to alleviate the extra work associated with an approach which at times breaks down.

CONCLUDING REMARKS

An influence coefficient matrix approach to the problem of longitudinal unconstrained vibrations of nonuniform multibranch beams is presented. The derivation is completely general and requires only basic parameter changes from one application to another. By making a change in variables the method can also be applied to torsional vibration problems. The derived matrix equations have been programed for the IBM 7094 electronic data processing system and have given excellent results in numerous applications.

A complete numerical example is given to illustrate the computations involved and a detailed illustration of the method applied to a launch vehicle is provided.

Comparison of the method with available exact solutions indicates that the accuracy of the solution is practically independent of cross-sectional variations but is contingent upon the chosen number of lumped masses in the analogous system. An approximate rule is given for determining the number of lumped masses to yield less than a 1-percent error in frequencies and mode shapes.

The influence coefficient matrix method is also compared with the stiffness matrix approach and is shown to be more accurate in the lower modes when there is a wide variation in the magnitudes of the frequencies of the system.

Langley Research Center,
National Aeronautics and Space Administration,
Langley Station, Hampton, Va., September 19, 1966,
124-11-05-30-23.

APPENDIX A

CLASSICAL WAVE EQUATION SOLUTION FOR BEAM WITH EXPONENTIALLY VARYING CROSS SECTION

For completeness, the solution for a beam with exponentially varying cross section is given. The classical wave equation for longitudinal vibrations is

$$\frac{\partial}{\partial x}\left(AE\,\frac{\partial u}{\partial x}\right) = \rho A\,\frac{\partial^2 u}{\partial t^2} \tag{A1}$$

where

$A = A(x)$ cross-sectional area

E modulus of elasticity

$\rho = \rho(x)$ mass density

$u = u(x,t)$ displacement

For undamped simple harmonic motion of frequency ω,

$$u(x,t) = \varphi(x)e^{i\omega t}$$

Substituting this expression into equation (A1) gives

$$AE\,\frac{d^2\varphi}{dx^2} + \frac{d(AE)}{dx}\,\frac{d\varphi}{dx} + \rho A\omega^2\varphi = 0 \tag{A2}$$

The beam under consideration has a cross-sectional area such that

$$A(x) = A(0)e^{2\beta x/L}$$

where L is the beam length and β is a constant.

Substituting this expression into equation (A2) gives

$$\frac{d^2\varphi}{dx^2} + \frac{2\beta}{L}\,\frac{d\varphi}{dx} + \frac{\rho\omega^2}{E}\,\varphi = 0 \tag{A3}$$

By letting $\lambda = \sqrt{\frac{\omega^2 L^2 \rho}{E} - \beta^2}$, the solution to equation (A3) is

$$\varphi(x) = e^{-\beta x/L}\left(A \cos \frac{\lambda x}{L} + B \sin \frac{\lambda x}{L}\right) \tag{A4}$$

where A and B are constants of integration.

If the free-free boundary conditions

$$\frac{d\varphi}{dx}(0) = \frac{d\varphi}{dx}(L) = 0$$

are utilized to evaluate A and λ, equation (A4) becomes

$$\varphi(x) = Ce^{-\beta x/L}\left(\cos \frac{n\pi x}{L} + \frac{\beta}{n\pi} \sin \frac{n\pi x}{L}\right) \tag{A5}$$

where

$C = \frac{n\pi B}{\beta}$ an arbitrary constant

$n = 0, 1, 2, \ldots$ an integer

Normalizing the displacement on $\varphi(0)$ gives

$$\frac{\varphi(x)}{\varphi(0)} = e^{-\beta x/L}\left(\cos \frac{n\pi x}{L} + \frac{\beta}{n\pi} \sin \frac{n\pi x}{L}\right) \tag{A6}$$

The frequency of vibration is determined from the evaluation of λ to be

$$\omega = \frac{\left(n^2\pi^2 + \beta^2\right)^{1/2}}{L}\sqrt{\frac{E}{\rho}} \tag{A7}$$

Equations (A6) and (A7) give the theoretical solution for the natural modes and frequencies of vibration. These equations reduce to the classical solution for a uniform beam if $\beta = 0$.

APPENDIX B

ROOT-MEAN-SQUARE PERCENT ERROR

To compare an approximate and theoretical curve by a single meaningful parameter is difficult since each curve consists of an infinite number of points. This difficulty is compounded by the more basic problem of how to initially aline the two curves.

The approximate mode shapes are normalized by an arbitrary constant. Therefore, adjusting this constant such that the error between the theoretical and approximate curves is a minimum yields a logical approach to alinement.

One method for determining an error parameter is to average the percent error of the points along the curve or to take the maximum value. This process, however, leads to a distorted accuracy picture due to the high percent error in the nodal point regions. A somewhat abstract but yet more realistic approach is to base the percent error on the average value of the theoretical curve. The derivation of such a parameter is included herein.

Let E^2 represent the mean square error between a typical theoretical curve and an approximate curve as depicted in sketch 11.

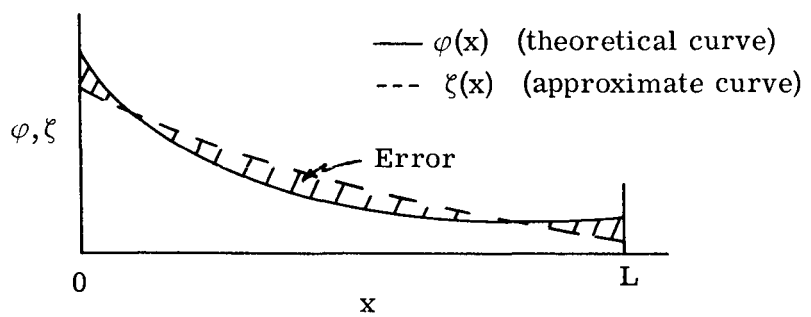

Sketch 11

The value of E^2 is then given as

$$E^2 = \frac{1}{L}\int_0^L \left[N\zeta(x) - \varphi(x)\right]^2 dx \tag{B1}$$

where N is an arbitrary normalizing coefficient of $\zeta(x)$. For the minimum value of E^2,

$$\frac{d\left(E^2\right)}{dN} = 0 \tag{B2}$$

Performing the differentiation of equation (B1) indicated by equation (B2) and solving for N gives

$$N = \frac{\int_0^L \varphi(x)\zeta(x)dx}{\int_0^L \zeta^2(x)dx} \tag{B3}$$

Equation (B3) can then be substituted into equation (B1) to evaluate E^2.

The mean square value of $\varphi(x)$ is

$$\overline{\varphi}(x)^2 = \frac{1}{L}\int_0^L \varphi^2(x)dx \tag{B4}$$

The root-mean-square (rms) percent error based on $\overline{\varphi}(x)$ is then

$$\text{rms percent error} = \frac{E}{\overline{\varphi}(x)} \times 100 \tag{B5}$$

Equation (B5) has been programed for the IBM 7094 electronic data processing system. Since the curve $\zeta(x)$ was defined by a limited number of points, a second-order interpolation scheme was used for the numerical integrations of the integrals in equations (B1), (B3), and (B4).

REFERENCES

1. Griffith, O. H.; and Cranch, E. T.: Torsional and Longitudinal Vibrations of Variable Section Bars. Paper No. 61-WA-75, Am. Soc. Mech. Engrs., 1961.

2. Lubkin, James L.; and Luke, Yudell L.: Frequencies of Longitudinal Vibration for a Slender Rod of Variable Section. J. Appl. Mech., vol. 20, no. 2, June 1953, pp. 173-177.

3. Wood, John D.: Survey on Missile Structural Dynamics. 7102-0041-NU-000, EM 11-11, (BSD-TN-61-42), Space Technol. Lab., Inc., June 1, 1961.

4. Batchelder, R. R.; and Wada, B. K.: Stiffness Matrix Structural Analysis. Tech. Mem. No. 33-75 (Contract No. NAS7-100), Jet Propulsion Lab., California Inst. Technol., Feb. 12, 1962, pp. 10-12.

5. Dudley, Winston M.: Analysis of Longitudinal Motions in Trains of Several Cars. J. Appl. Mech., vol. 8, no. 4, Dec. 1941, pp. A-141 – A-151.

6. Timoshenko, S.; and Young, D. H.: Vibration Problems in Engineering. Third ed., D. Van Nostrand Co., Inc., c.1955.

7. Wingate, Robert T.: Matrix Analysis of Natural Longitudinal Vibrations in Free-Free Nonuniform Multibranch Beams. M.S. Thesis, Univ. of Virginia, 1964.

8. Scanlan, Robert H.; and Rosenbaum, Robert: Introduction to the Study of Aircraft Vibration and Flutter. The Macmillan Co., 1951, pp. 168-173.

9. Timoshenko, S.; and Goodier, J. N.: Theory of Elasticity. Second ed., McGraw-Hill Book Co., Inc., 1951, p. 264.

10. Bodewig, E.: Matrix Calculus. Second rev. ed., Interscience Publ., Inc., 1959.

11. Alley, Vernon L., Jr.; and Gerringer, A. Harper: A Matrix Method for the Determination of the Natural Vibrations of Free-Free Unsymmetrical Beams With Application to Launch Vehicles. NASA TN D-1247, 1962, pp. 12-16.

12. Browne, Edward Tankard: Introduction to the Theory of Determinants and Matrices. Univ. of North Carolina Press, c.1958.

13. Dickson, Leonard Eugene: New First Course in the Theory of Equations. John Wiley & Sons, Inc., 1939, p. 131.

TABLE 1.- VEHICLE MASS DISTRIBUTION

(a) U.S. Customary Units

x, in.	m, $\frac{\text{lbf-sec}^2}{\text{in}^2}$	x, in.	m, $\frac{\text{lbf-sec}^2}{\text{in}^2}$	x, in.	m, $\frac{\text{lbf-sec}^2}{\text{in}^2}$
-15.8	0.036808	456.9	0.004788	496.299	0.051756
0	.046624	468.449	.004788	497.299	.051756
19.1	.046624	468.449	.027562	497.299	.045316
19.1	.071398	468.949	.027562	520.789	.045316
29.6	.071398	468.949	.019565	520.789	.046558
29.6	.049883	469.199	.019565	522.199	.046558
102.2	.049883	469.199	.021480	522.199	.004710
102.2	.059536	469.389	.021480	526.789	.004710
173.3	.059536	469.389	.023784	526.789	.0159318
173.3	.100380	469.949	.023551	531.099	.0159318
177.3	.100380	469.949	.028338	531.099	.027685
177.3	.007668	470.949	.028080	533.049	.027685
186.4	.007668	470.949	.034161	533.049	.005435
186.4	.018549	471.199	.034032	537.269	.005435
188.4	.018549	471.199	.018401	537.269	.005823
188.4	.012378	474.949	.017728	538.809	.005564
195.9	.012378	474.949	.011232	538.809	.006185
195.9	.025331	476.199	.011077	540.199	.005900
207.4	.025331	476.199	.006315	545.199	.005176
207.4	.023834	476.749	.006211	548.309	.004790
214.9	.023834	476.749	.008463	548.309	.008851
214.9	.024559	482.285	.008230	552.0	.00880
317.1	.024559	482.285	.014880	554.059	.008644
317.1	.044689	482.749	.014880	554.059	.001941
322.1	.044689	482.749	.012681	559.949	.001579
322.1	.013808	483.199	.012681	559.949	.000924
331.4	.013808	483.199	.011439	562.0	.00070
331.4	.025466	485.999	.011439	565.199	.000655
345.4	.025466	488.285	.011827	566.0	.000500
345.4	.022530	488.285	.005952	573.46	.000466
350.4	.022530	488.785	.006315	573.46	.001633
350.4	.024559	488.785	.018245	577.629	.001633
451.9	.024559	490.799	.019358	577.629	.001568
451.9	.044689	490.799	.045031	577.629	0
456.9	.044689	496.299	.045031		

TABLE 1.- VEHICLE MASS DISTRIBUTION – Concluded

(b) SI Units

x, m	m, $\frac{N\text{-}sec^2}{m^2}$	x, m	m, $\frac{N\text{-}sec^2}{m^2}$	x, m	m, $\frac{N\text{-}sec^2}{m^2}$
-0.4013	253.782	11.4783	169.328	12.4663	133.469
0	321.461	11.4783	308.120	12.4663	310.478
.4851	321.461	11.6053	308.120	12.6060	310.478
.4851	492.272	11.6053	33.012	12.6060	356.845
.7518	492.272	11.8986	33.012	12.6314	356.845
.7518	343.931	11.8986	190.033	12.6314	312.443
2.5959	343.931	11.9113	190.033	13.2280	312.443
2.5959	410.486	11.9113	134.896	13.2280	321.006
4.4018	410.486	11.9177	134.896	13.2638	321.006
4.4018	692.096	11.9177	148.099	13.2638	32.474
4.5034	692.096	11.9225	148.099	13.3804	32.474
4.5034	52.869	11.9225	163.985	13.3804	109.846
4.7346	52.869	11.9367	162.378	13.4899	109.846
4.7346	127.891	11.9367	195.384	13.4899	190.881
4.7854	127.891	11.9621	193.605	13.5394	190.881
4.7854	85.343	11.9621	235.532	13.5394	37.473
4.9759	85.343	11.9685	234.642	13.6466	37.473
4.9759	174.651	11.9685	126.870	13.6466	40.148
5.2680	174.651	12.0637	122.230	13.6857	38.362
5.2680	164.330	12.0637	77.442	13.6857	42.644
5.4585	164.330	12.0955	76.373	13.7210	40.679
5.4585	169.328	12.0955	43.540	13.8480	35.687
8.0543	169.328	12.1094	42.823	13.9270	33.026
8.0543	308.120	12.1094	58.350	13.9270	61.025
8.1813	308.120	12.2500	56.744	14.0208	60.674
8.1813	95.203	12.2500	102.594	14.0731	59.598
8.4176	95.203	12.2618	102.594	14.0731	13.383
8.4176	175.582	12.2618	87.432	14.2227	10.887
8.7732	175.582	12.2733	87.432	14.2227	6.371
8.7732	155.339	12.2733	78.869	14.2748	4.826
8.9002	155.339	12.3444	78.869	14.3560	4.516
8.9002	169.328	12.4024	81.544	14.3764	3.447
		12.4024	41.038	14.5659	3.213
		12.4151	43.540	14.5659	11.259
		12.4151	125.795	14.6718	10.811
				14.6718	0

TABLE 2.- VEHICLE AXIAL EXTENSIONAL COEFFICIENT

(a) U.S. Customary Units

x, in.	AE, lbf	x, in.	AE, lbf	x, in.	AE, lbf
0	295.1×10^6	171.976	1041.3×10^6	345.4	199.1×10^6
1.476	295.1	172.976	1041.3	345.4	612.0
1.476	280.3	172.976	2449.2	346.5	199.1
6.476	280.3	176.976	2449.2	349.0	336.7
6.476	309.4	176.976	39.0	349.0	730.1
9.076	309.4	185.356	39.0	350.4	730.1
9.076	1201.7	185.356	78.0	350.4	195.0
11.376	1201.7	187.956	78.0	352.3	70.5
11.376	504.4	187.956	112.8	452.3	70.5
13.976	504.4	193.582	112.8	453.9	184.5
13.976	613.6	193.582	135.2	456.0	529.1
15.976	613.6	198.5	135.2	456.9	529.1
15.976	699.9	198.5	369.2	456.9	187.8
17.976	699.9	199.3	369.2	458.8	187.8
17.976	2350.4	199.3	130.0	458.8	75.4
20.776	2350.4	203.756	130.0	461.4	75.4
20.776	841.88	203.756	118.6	461.4	707.2
24.176	841.88	205.916	118.6	461.7	707.2
24.176	689.3	205.916	169.0	461.7	75.4
25.376	689.3	208.7	169.0	465.6	75.4
25.376	316.7	208.7	442.0	467.6	210.6
25.776	316.7	209.556	442.0	467.6	190.9
25.776	576.4	209.556	280.8	468.9	452.4
28.476	576.4	212.256	280.8	468.9	452.4
28.476	316.7	212.256	730.1	469.699	870.7
32.376	316.7	213.656	730.1	470.011	870.7
32.376	576.4	213.656	137.8	470.011	162.8
37.376	576.4	215.556	137.8	471.824	98.5
37.376	316.7	215.556	70.5	471.824	33.46
100.776	316.7	315.556	70.5	489.699	33.46
100.776	576.4	315.556	130.0	489.699	182.16
103.776	576.4	317.156	130.0	491.035	182.16
103.776	316.7	317.156	431.6	491.035	25.74
161.276	316.7	320.156	431.6	492.0	25.74
161.276	576.4	320.156	213.2	492.0	4.45
164.276	576.4	322.156	213.2	537.268	2.91
164.276	316.7	322.156	71.42	543.268	1.91
169.376	316.7	324.7	98.64	549.268	1.37
169.376	841.9	332.2	136.83	553.627	.782
171.876	841.9	335.2	425.6	559.627	.398
171.876	316.7	336.0	136.83	571.62	.169
171.976	316.7	342.0	112.6	574.327	4.62
				577.629	0

TABLE 2.- VEHICLE AXIAL EXTENSIONAL COEFFICIENT – Concluded

(b) SI Units

x, m	AE, N	x, m	AE, N	x, m	AE, N
0	131.266×10^7	4.3936	463.191×10^7	8.8011	88.564×10^7
.0375	131.266	4.3936	1089.453	8.8646	149.771
.0375	124.683	4.4952	1089.453	8.8646	324.763
.1645	124.683	4.4952	17.348	8.9002	324.763
.1645	137.627	4.7080	17.348	8.9002	86.740
.2305	137.627	4.7080	34.696	8.9484	31.360
.2305	534.540	4.7741	34.696	11.4884	31.360
.2890	534.540	4.7741	50.176	11.5291	82.069
.2890	224.367	4.9170	50.176	11.5824	235.354
.3550	224.367	4.9170	60.140	11.6053	235.354
.3550	272.942	5.0419	60.140	11.6053	83.537
.4058	272.942	5.0419	164.228	11.6535	83.537
.4058	311.329	5.0622	164.228	11.6535	33.539
.4566	311.329	5.0622	57.827	11.7196	33.539
.4566	1045.504	5.1754	57.827	11.7196	314.577
.5277	1045.504	5.1754	52.756	11.7272	314.577
.5277	374.485	5.2303	52.756	11.7272	33.539
.6141	374.485	5.2303	75.174	11.8262	33.539
.6141	306.614	5.3010	75.174	11.8770	93.679
.6446	306.614	5.3010	196.610	11.8770	84.916
.6446	140.874	5.3227	196.610	11.9101	201.236
.6548	140.874	5.3227	124.905	11.9101	201.236
.6548	256.394	5.3913	124.905	11.9304	387.305
.7233	256.394	5.3913	324.763	11.9383	387.305
.7233	140.874	5.4269	324.763	11.9383	72.417
.8224	140.874	5.4269	61.296	11.9843	43.815
.8224	256.394	5.4751	61.296	11.9843	14.884
.9494	256.394	5.4751	31.360	12.4384	14.884
.9494	140.874	8.0151	31.360	12.4384	81.028
2.5597	140.874	8.0151	57.827	12.4723	81.028
2.5597	256.394	8.0558	57.827	12.4723	11.450
2.6359	256.394	8.0558	191.984	12.4968	11.450
2.6359	140.874	8.1320	191.984	12.4968	1.979
4.0964	140.874	8.1320	94.836	13.6466	1.294
4.0964	256.394	8.1828	94.836	13.7990	.850
4.1726	256.394	8.1828	31.769	13.9514	.609
4.1726	140.874	8.2474	43.877	14.0621	.3478
4.3022	140.874	8.4379	60.865	14.2145	.1770
4.3022	374.494	8.5141	189.315	14.5191	.0752
4.3656	374.494	8.5344	60.865	14.5879	2.055
4.3656	140.874	8.6868	50.087	14.6718	0
4.3682	140.874	8.7732	88.564		
4.3682	463.191	8.7732	272.230		

TABLE 3.- PAYLOAD PHYSICAL CHARACTERISTICS

(a) U.S. Customary Units

x, in.	m_x, $\frac{\text{lbf-sec}^2}{\text{in}^2}$	AE, lbf
472.32	0.0200	2.0000×10^6
532.32	.0200	2.0000

(b) SI Units

x, m	m_x, $\frac{\text{N-sec}^2}{\text{m}^2}$	AE, N
11.997	137.8951	0.8896×10^7
13.521	137.8951	.8896

TABLE 4.- COMPARISON OF SOLUTIONS TO EIGENVALUE PROBLEMS OBTAINED FROM BOTH STIFFNESS AND FLEXIBILITY APPROACHES

Mode \ η	2	4	5	6	7	8	10	Method[a]
Frequency ratio, ω/ω_{ref} [b]								
1	0.99952	0.99989	0.99965	0.999652	0.94111	0.80404	80.404	I
	.99952	.99996	.99982	2158.3	6825.3	21 580.	1.5×10^5	II
	.99952	.99999	1.0	1.0	1.0	1.0	1.0	III
	.99952	.99999	1.0	1.0	1.0	1.0	1.0	IV
2	0.99943	1.0	0.99998	0.99962	2.0107	18.001	1798.8	I
	.99943	1.0	1.0	1.1202	14.656	.97744	1.1656	II
	.99943	1.0	1.0	1.0	1.0	1.0	1.0	III
	.99943	1.0	1.0	1.0	1.0	1.0	1.0	IV
3	0.99979	0.99999	0.99999	0.99992	1.6042	13.124	1310.2	I
	.99979	.99999	.99999	.99999	.99988	.99844	.99984	II
	.99979	.99999	.99999	1.0	1.0	1.0	1.0	III
	.99979	.99999	1.0	1.0	1.0	1.0	1.0	IV
4	1.0013	1.0	1.0	1.0	1.0	1.0	1.0	I
	1.0013	1.0	1.0	1.0	1.0	1.0	1.0	II
	1.0013	(c)	(c)	(c)	(c)	(c)	(c)	III
	1.0013	1.0	.99932	1.0027	.97831	(d)	(d)	IV
Reference frequency, ω_{ref}								
1	0.65523	0.65523	0.65523	0.65523	0.65523	0.65523	0.65523	
2	1.3257	1.3257	1.3257	1.3257	1.3257	1.3257	1.3257	
3	1.8202	1.8202	1.8202	1.8202	1.8202	1.8202	1.8202	
4	14.142	141.42	447.21	1414.2	4472.1	14 142.1	141 421.	

[a] I: Givens solution (ref. 10, pp. 336-340) to stiffness matrix.
II: Iteration and sweeping solution (ref. 11) to stiffness matrix.
III: Iteration and sweeping solution to flexibility matrix.
IV: Givens solution to flexibility matrix.

[b] ω is the calculated modal frequencies of 5 mass system;
ω_{ref} is the reference modal frequencies calculated from degenerate 4 mass and 2 mass systems.

[c] Solution failed to converge.

[d] Imaginary (complex) frequency.

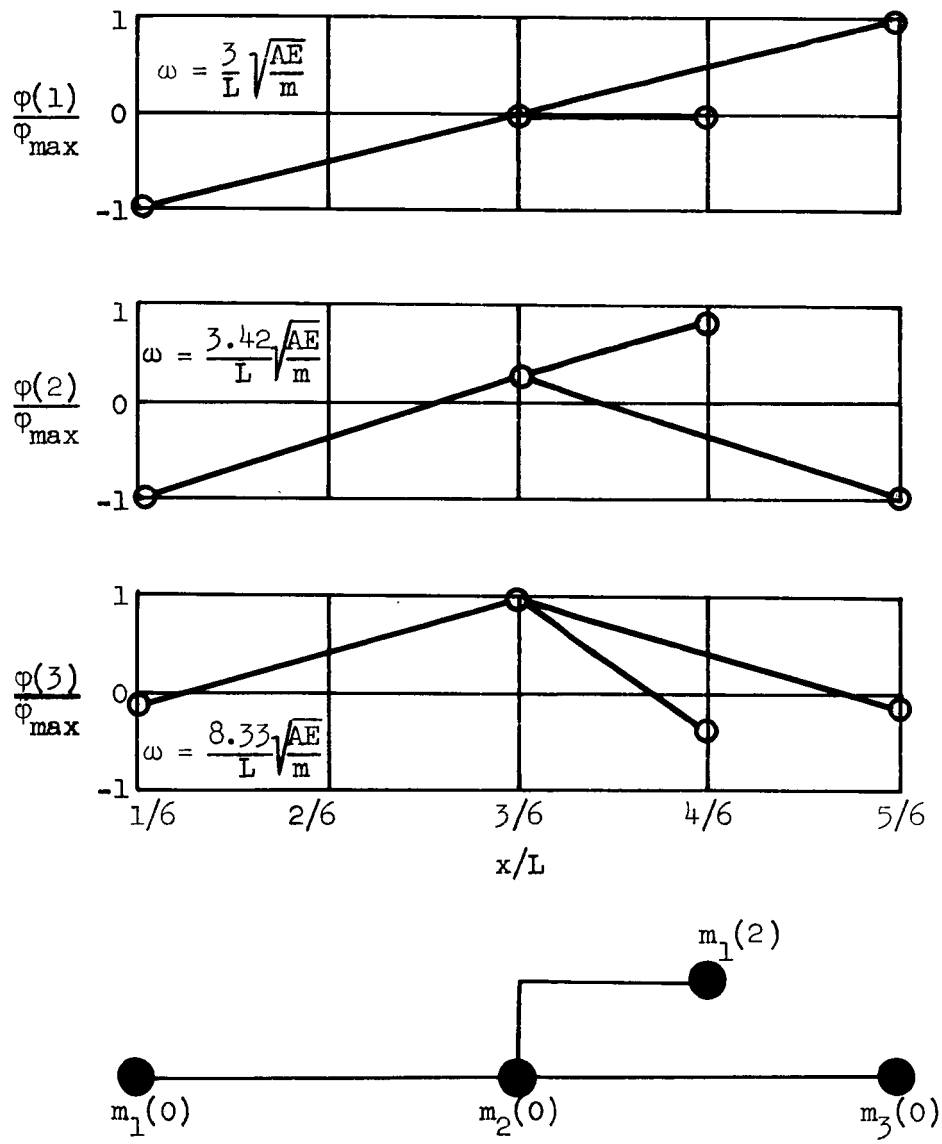

Figure 1.- Numerical example natural modes.

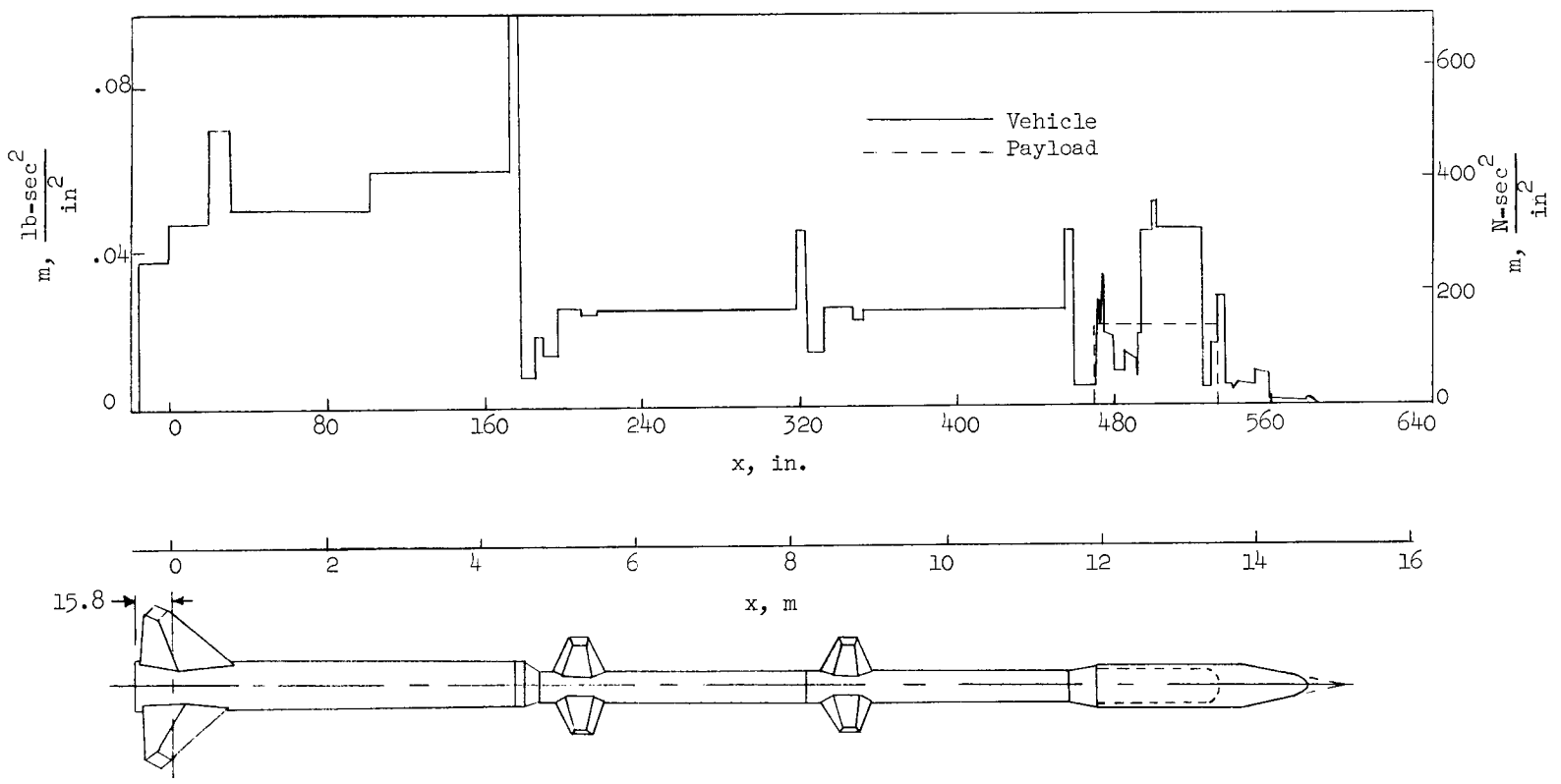

Figure 2.- Rocket-vehicle mass per inch. m values from tables 1 and 3.

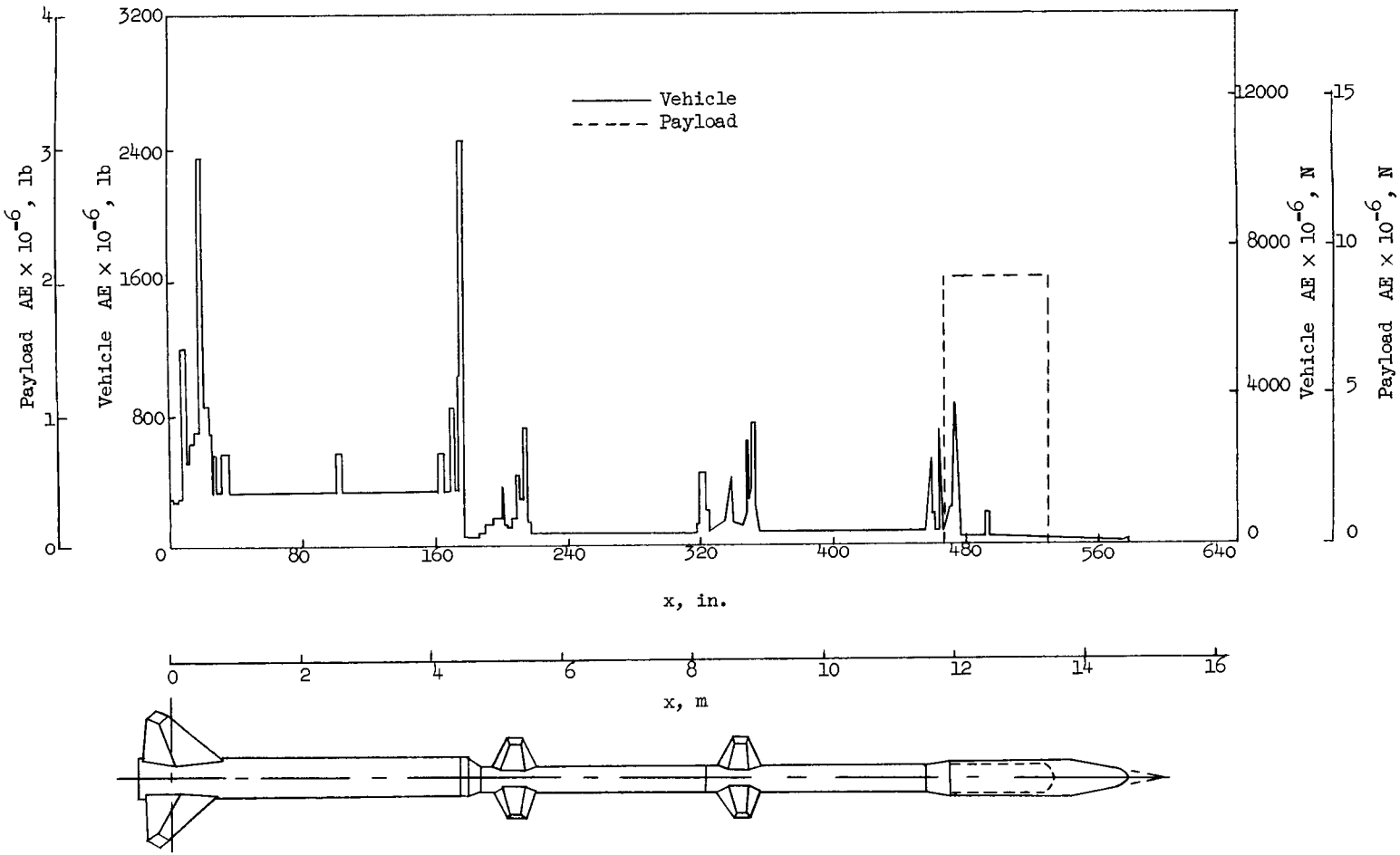

Figure 3.- Rocket-vehicle axial extensional coefficient. AE values from tables 2 and 3.

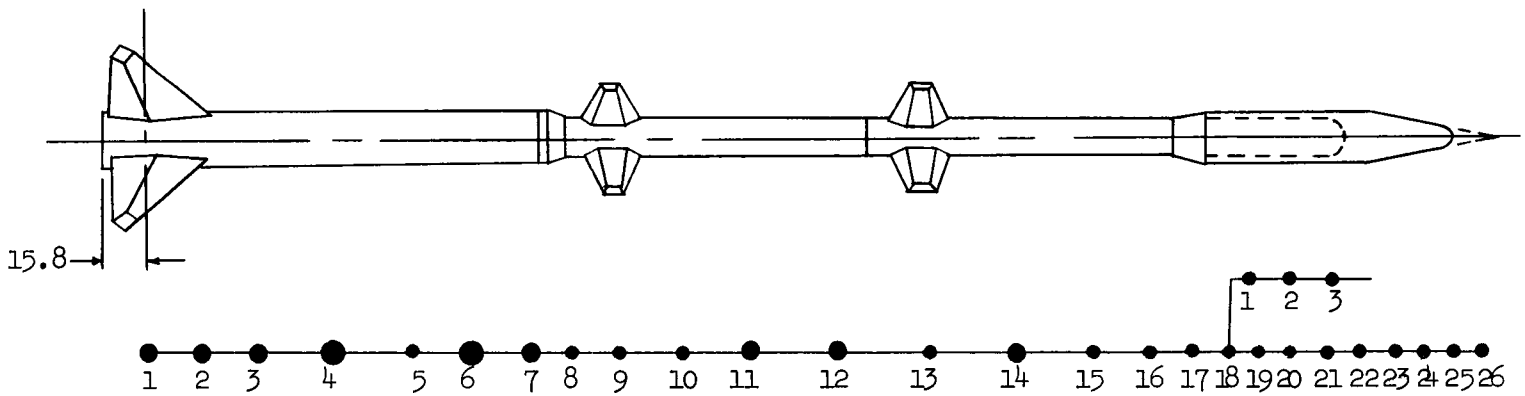

Vehicle				Payload		
	x/L =	m/M =		x/L =	m/M =	
1	0	0.056577		.826	.020	18
2	0.037664	.051814		.860	.020	19
3	.073702	.063030		.894	.020	20
4	.133536	.136304				21
5	.193456	.017427				22
6	.232832	.116297				23
7	.281915	.050132				24
8	.308160	.022619				25
9	.349248	.038751				26
10	.393760	.017972				
11	.445120	.053916				
12	.512402	.052356				
13	.583278	.035264				
14	.648420	.050921				
15	.708768	.038340				
16	.754906	.026239				
17	.775330	.014271				
18	.808612	.009953				
19	.836226	.019465				
20	.862249	.028079				
21	.884128	.028110				
22	.906555	.005990				
23	.930078	.005634				
24	.949749	.001406				
25	.965482	.000128				
26	.981764	.000454				

Figure 4.- Rocket-vehicle analogous discrete mass system. $M = 20.497 \frac{\text{lb-sec}^2}{\text{in.}} \left(3589.678 \frac{\text{N-sec}^2}{\text{m}}\right)$; L = 577.629 in. (14.672 m).

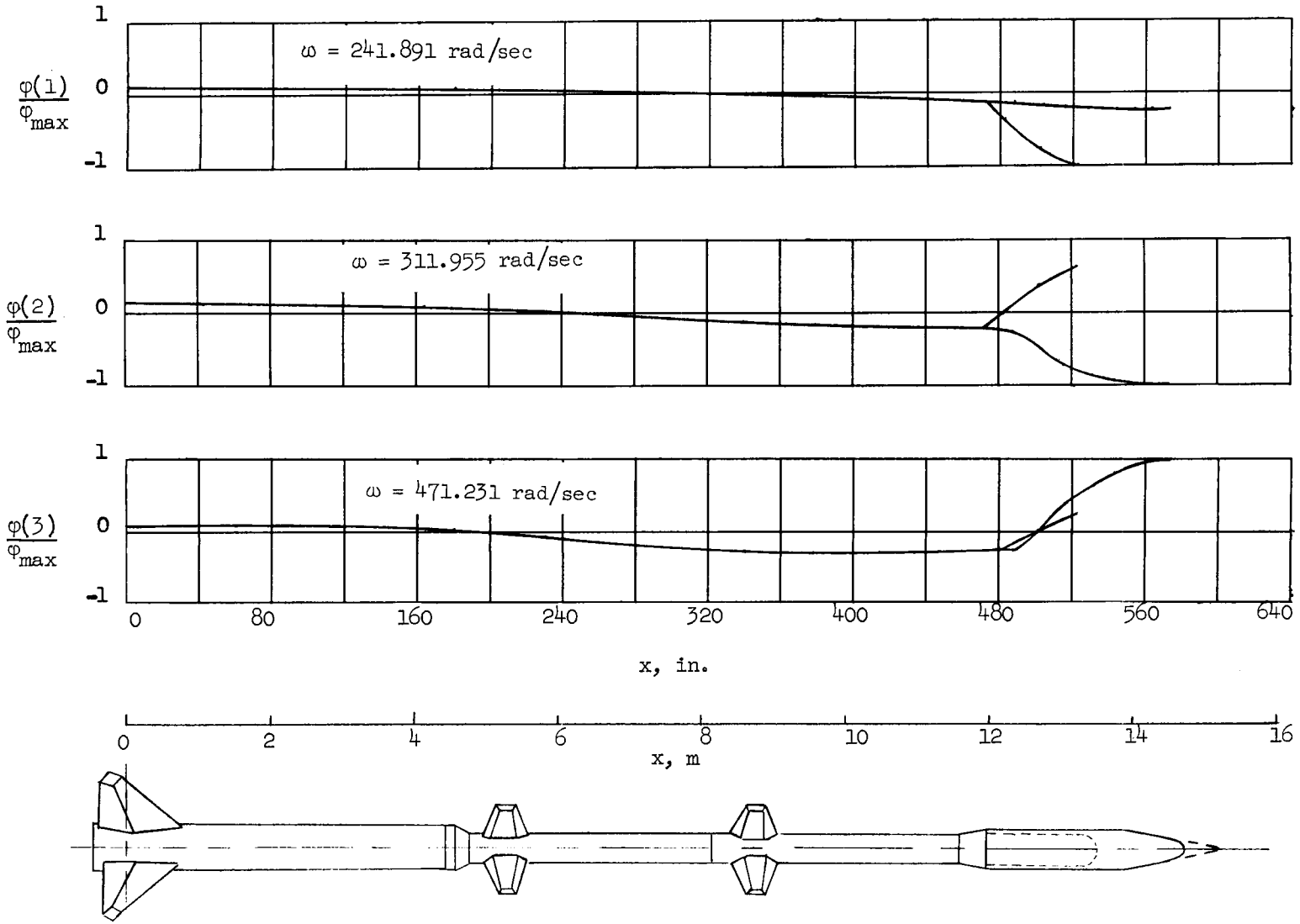

Figure 5.- Rocket-vehicle longitudinal natural modes.

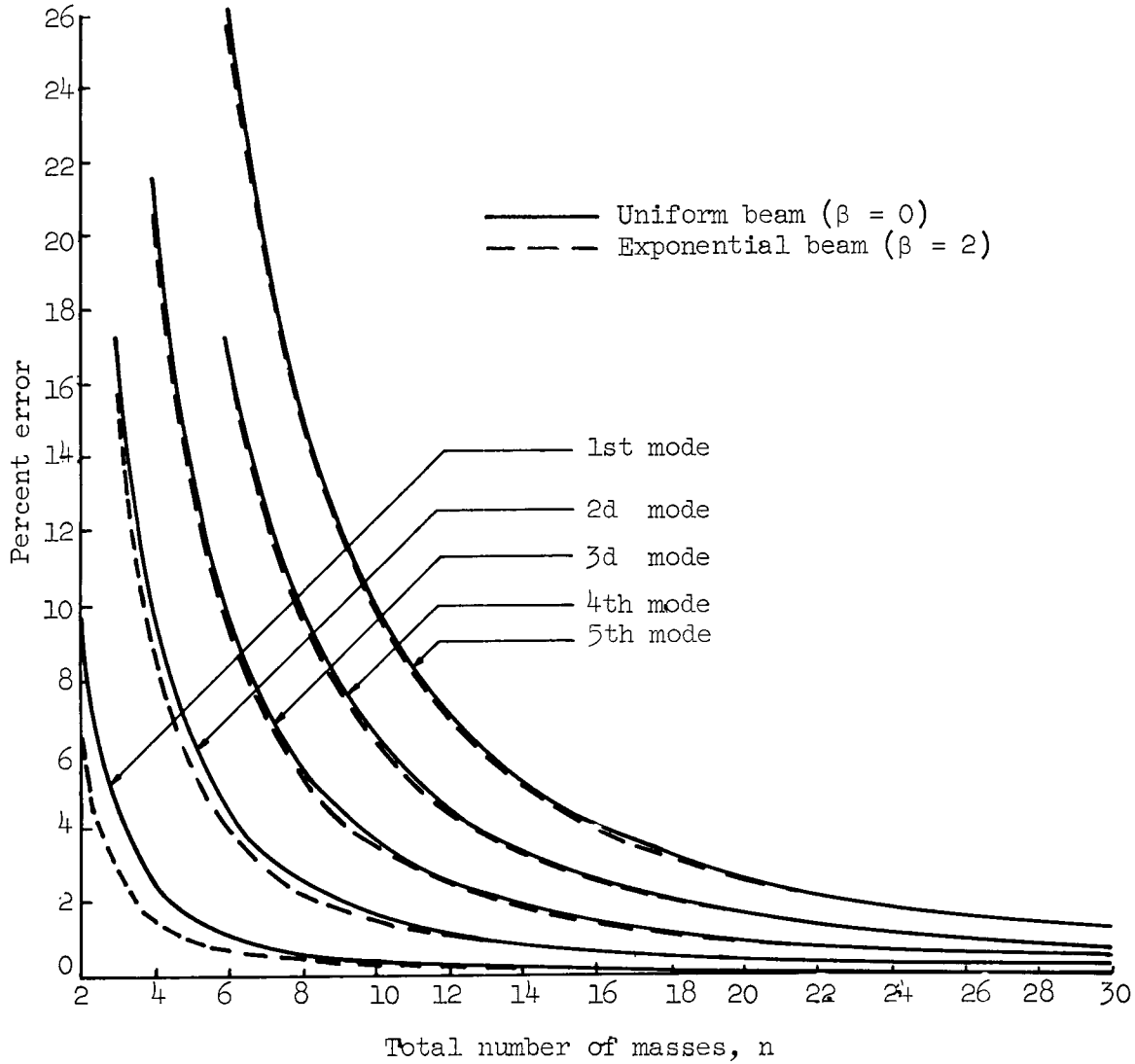

Figure 6.- Frequency percent error as a function of total number of lumped masses.

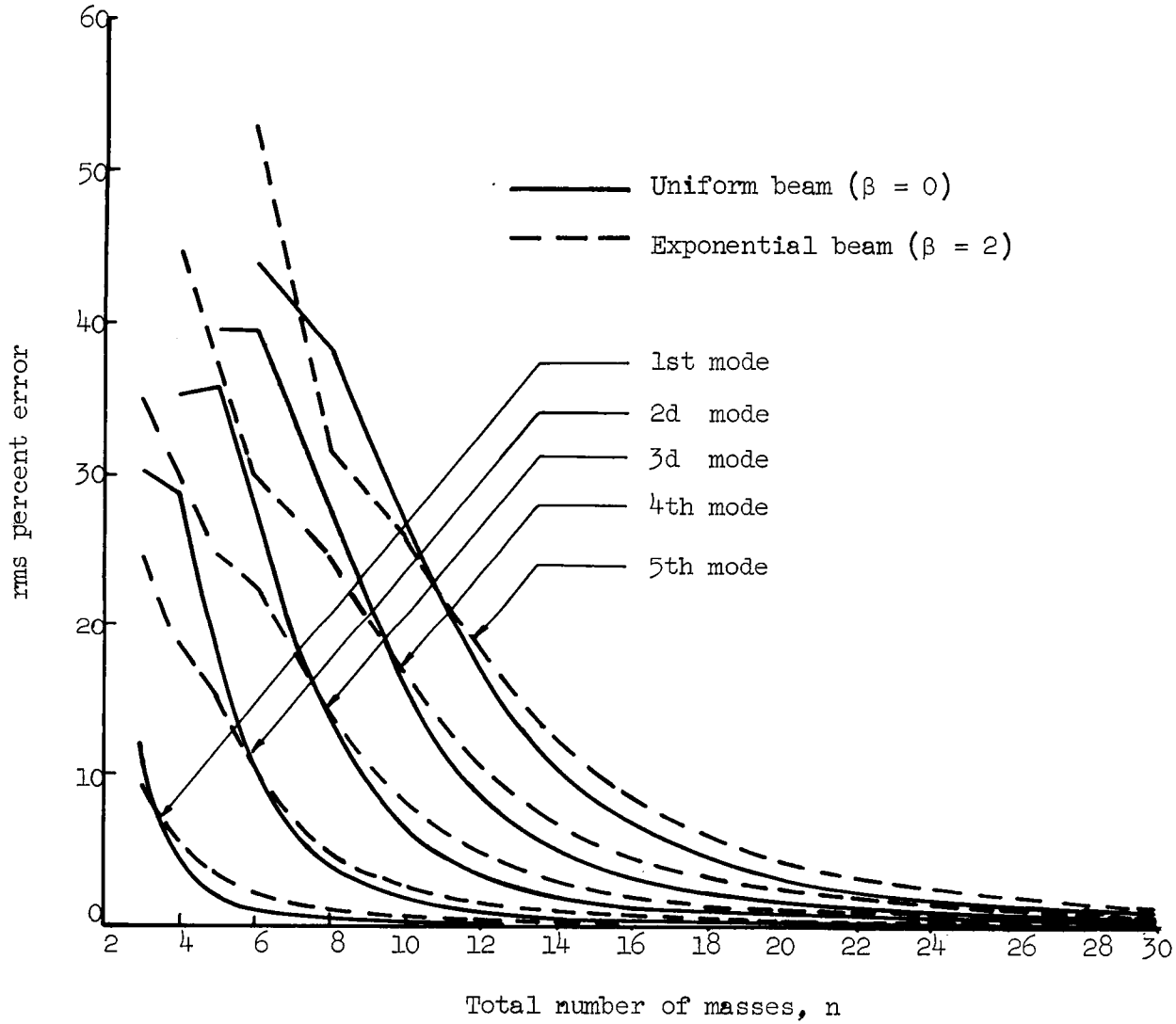

Figure 7.- Mode-shape rms percent error as a function of total number of lumped masses.

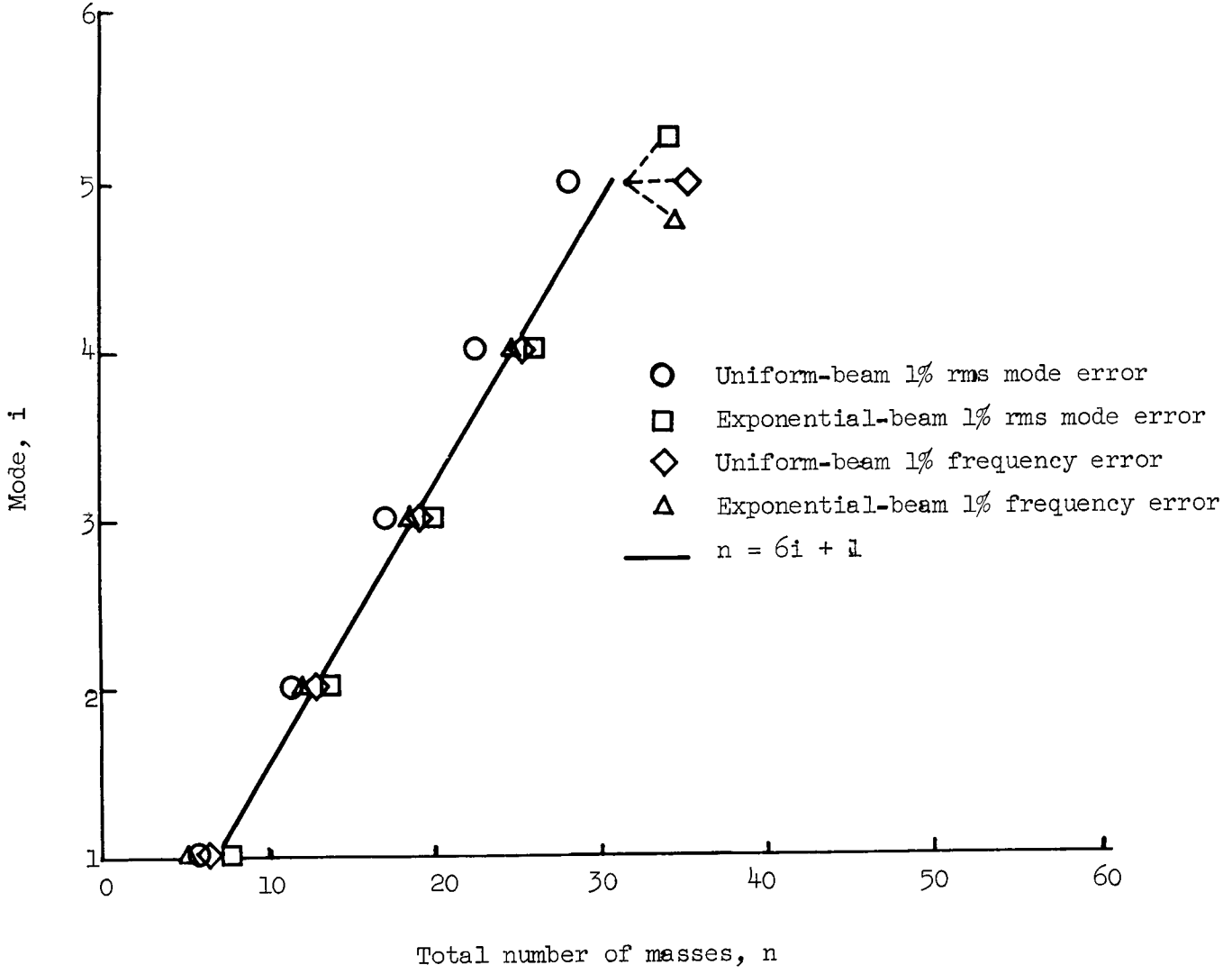

Figure 8.- Flexible mode number as a function of total number of masses for a 1-percent mode-shape error or frequency error.

04172
58 ap
3-2-67

"The aeronautical and space activities of the United States shall be conducted so as to contribute . . . to the expansion of human knowledge of phenomena in the atmosphere and space. The Administration shall provide for the widest practicable and appropriate dissemination of information concerning its activities and the results thereof."

—NATIONAL AERONAUTICS AND SPACE ACT OF 1958

NASA SCIENTIFIC AND TECHNICAL PUBLICATIONS

TECHNICAL REPORTS: Scientific and technical information considered important, complete, and a lasting contribution to existing knowledge.

TECHNICAL NOTES: Information less broad in scope but nevertheless of importance as a contribution to existing knowledge.

TECHNICAL MEMORANDUMS: Information receiving limited distribution because of preliminary data, security classification, or other reasons.

CONTRACTOR REPORTS: Technical information generated in connection with a NASA contract or grant and released under NASA auspices.

TECHNICAL TRANSLATIONS: Information published in a foreign language considered to merit NASA distribution in English.

TECHNICAL REPRINTS: Information derived from NASA activities and initially published in the form of journal articles.

SPECIAL PUBLICATIONS: Information derived from or of value to NASA activities but not necessarily reporting the results of individual NASA-programmed scientific efforts. Publications include conference proceedings, monographs, data compilations, handbooks, sourcebooks, and special bibliographies.

Details on the availability of these publications may be obtained from:

SCIENTIFIC AND TECHNICAL INFORMATION DIVISION

NATIONAL AERONAUTICS AND SPACE ADMINISTRATION

Washington, D.C. 20546